



Symmetry breakage in the vertebrate embryo: When does it happen and how does it work?



Martin Blum^{a,*}, Axel Schweickert^a, Philipp Vick^a, Christopher V.E. Wright^b,
Michael V. Danilchik^c

^a University of Hohenheim, Institute of Zoology (220), Garbenstrasse 30, D-70593 Stuttgart, Germany

^b Department of Cell and Developmental Biology, Vanderbilt University, Nashville, TN 37232-0494, USA

^c Department of Integrative Biosciences, Oregon Health & Science University, Portland, OR 97239-3098, USA

ARTICLE INFO

Article history:

Received 25 February 2014

Received in revised form

8 June 2014

Accepted 17 June 2014

Available online 24 June 2014

Keywords:

Left–right asymmetry

Cilia

Leftward flow

Ion-flux model

Symmetry breakage

ABSTRACT

Asymmetric development of the vertebrate embryo has fascinated embryologists for over a century. Much has been learned since the asymmetric Nodal signaling cascade in the left lateral plate mesoderm was detected, and began to be unraveled over the past decade or two. When and how symmetry is initially broken, however, has remained a matter of debate. Two essentially mutually exclusive models prevail. Cilia-driven leftward flow of extracellular fluids occurs in mammalian, fish and amphibian embryos. A great deal of experimental evidence indicates that this flow is indeed required for symmetry breaking. An alternative model has argued, however, that flow simply acts as an amplification step for early asymmetric cues generated by ion flux during the first cleavage divisions. In this review we critically evaluate the experimental basis of both models. Although a number of open questions persist, the available evidence is best compatible with flow-based symmetry breakage as the archetypical mode of symmetry breakage.

© 2014 The Authors. Published by Elsevier Inc. This is an open access article under the CC BY-NC-ND license (<http://creativecommons.org/licenses/by-nc-nd/3.0/>).

Introduction

Establishment of left–right asymmetry of animal body plans is of the utmost importance for embryonic development and adult health. During vertebrate embryogenesis, the cardiovascular system, the organs of the chest and abdomen, and even the brain, develop morphological and/or functional asymmetries (Aizawa, 2013; Burn and Hill, 2009; Franco et al., 2014; Perloff, 2011; Roussigne et al., 2012). Developmental defects in laterality specification and asymmetric morphogenesis are sometimes compatible with embryogenesis, and occasionally, fully mirror-image individuals develop to term (Bartram et al., 2005; Peeters and Devriendt, 2006; Shiraiishi and Ichikawa, 2012; Sutherland and Ware, 2009). Left–right (L–R) defects are often much less pervasive and usually strike organs at random, resulting in severe visceral misalignment, organ malformations and malfunctions (Burdine and Caspary, 2013; Hirokawa et al., 2012; Yoshida and Hamada, 2014). Asymmetric organ morphogenesis is preceded by an asymmetric signaling cascade, which initiates during neurulation in the left lateral plate mesoderm (LPM). This so-called Nodal cascade

consists of the TGF β -type growth factor Nodal, its secreted feedback repressor Lefty (also known as Antivin) and the homeodomain transcription factor Pitx2 (Marjoram and Wright, 2011; Schier, 2009; Shen, 2007). Expression of this cascade is both necessary and sufficient to induce the correct asymmetric placement of organs (situs solitus) (Hamada et al., 2002; Hirokawa et al., 2012).

How the Nodal cascade becomes asymmetrically expressed constitutes a conceptual cell-biological problem, because zygotes typically lack recognizable morphological or functional asymmetries that could initiate it. Brown and Wolpert (1990) proposed the concept of an intrinsic biochemical-structural chirality (represented in their model by an “F-molecule”), even though uniformly distributed, such a molecule would operate by undergoing chiral alignment against the A–P and D–V axes of the embryo. Then other molecular interactions feeding off the deduced L–R vector would eventually lead (via an unknown number of steps) to the morphogenetic process of asymmetric organ development (Brown and Wolpert, 1990). Amongst the animals classified as the bilateria, two cytoskeleton-dependent chiralities have been identified, whose mechanism of action fulfill the conceptual nature of the F-molecule hypothesis (though not being single molecules in the initial invocation of the model). Interestingly, although expressed at two different developmental stages, both of these instances

* Corresponding author.

E-mail address: martin.blum@uni-hohenheim.de (M. Blum).

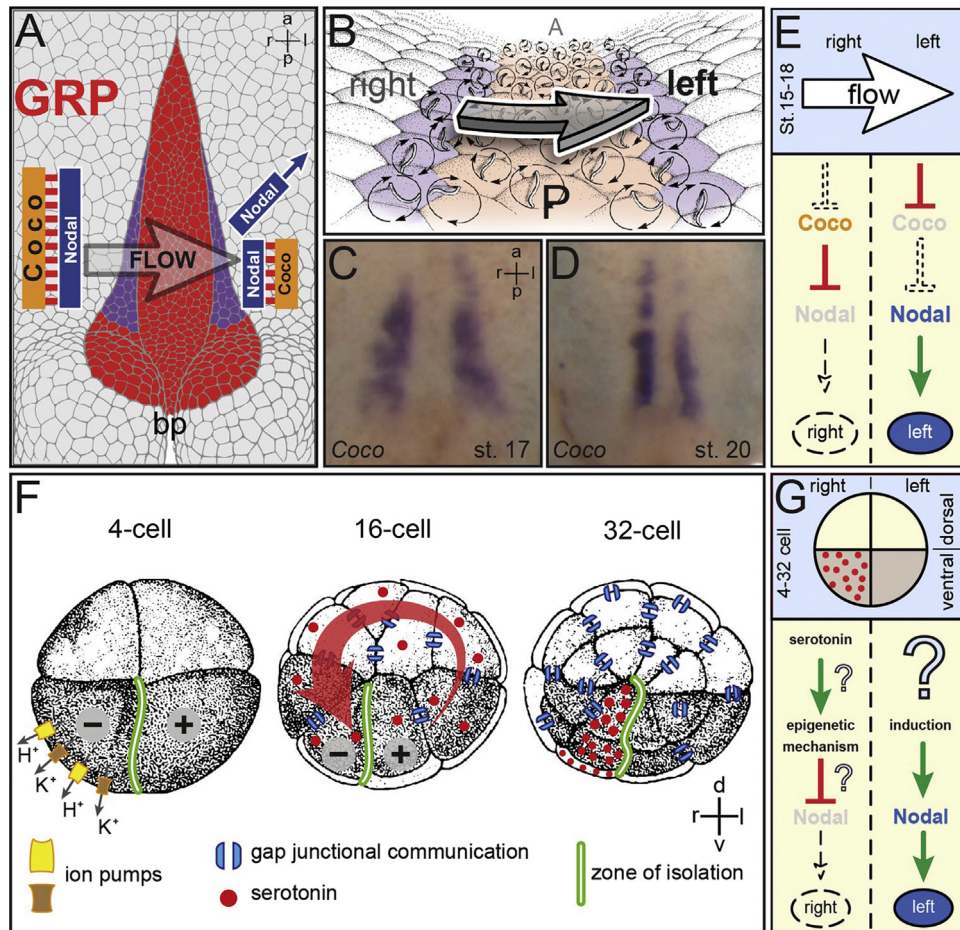


Fig. 1. Prevailing models of symmetry breakage in the frog *Xenopus*. (A–E) Leftward flow. (A) Schematic representation of a stage 17 archenteron roof in ventral perspective. Flow occurs from the right to the left side of the ciliated gastrocoel roof plate (GRP; red). *Nodal* and *Coco* are co-expressed at the lateral GRP margins on both sides (purple). Flow represses *Coco*, activating *Nodal* by release of repression. bp, blastopore. (B) GRP at higher magnification. Polarized and flow-producing cilia at the GRP center are bordered by *Nodal/Coco*-positive cells (purple) which harbor unpolarized, sensory cilia. (C and D) *Coco* expression during (C) and following (D) leftward flow. Note the decrease in signal intensity on the left at post-flow stage 20 (D). (E) Schematic depiction of events on the left and right side leading up to asymmetric *Nodal* cascade induction in the left lateral plate mesoderm (LPM). (F and G) Ion-flux. (F) Asymmetrically expressed ion pumps create a voltage gradient in the 4-cell embryo which initiates the electrogenic transfer of serotonin through gap junctional communication to the ventral-right lineage at the 32-cell stage. Serotonin accumulates in this lineage because the ventral midline is devoid of GJC. (G) Schematic depiction of events on the left and right side leading up to asymmetric *Nodal* cascade induction in the left LPM. Question marks indicate unproven interactions and mechanisms.

result in asymmetric activation of the *Nodal* pathway. In spirally cleaving snail embryos, asymmetric positioning of the spindle apparatus during cleavage induces *Nodal* asymmetry, ostensibly by repositioning maternally synthesized factors (Grande and Patel, 2009). In embryos of most vertebrates, including fish, frogs and mammals, chiral rotation of cilia polarized to the posterior pole of cells produces a vectorial leftward flow of extracellular fluids. This flow is necessary and sufficient for *Nodal*-dependent symmetry breakage (Fig. 1A–E; Basu and Brueckner, 2008; Blum et al., 2009b; Hirokawa et al., 2012), and substantial enough to sweep fluorescent latex microbeads across from one side of the ciliated epithelium to the other (Essner et al., 2005; Kramer-Zucker et al., 2005; Nonaka et al., 1998; Okada et al., 2005; Schweickert et al., 2007). Although both mechanisms lead to asymmetric *Nodal* activity, they seem to have little else in common, raising the question as to why and how flow-type symmetry breakage has evolved. We have recently addressed this problem in a hypothesis article (Blum et al., 2014), and will not repeat this issue here. One major difference between the two strategies is that one (spiral cleavage in spiralian protostomes) is determined maternally and acts during very early cleavage stages, while the other (leftward flow) operates much later, and depends on zygotic gene expression during neurula stages.

Although most of the vertebrates examined so far utilize cilia-generated flow to initiate the asymmetric *Nodal* cascade, two alternative strategies have also been observed. First, in the chick, large-scale whole-cell repositioning during gastrulation results in a significant asymmetry in the morphology of Hensen's node, and this appears to play a role in the asymmetric expression of specific intercellular signaling molecules (Dathe et al., 2002; Gros et al., 2009; Wetzel, 1929). Second, in amphibians, asymmetric localization of determinants has been proposed to act during early cleavage stages (Fig. 1F and G; for a recent review see Vandenberg and Levin, 2013). According to this view, cytoskeletal motor proteins asymmetrically transport a maternal deposit of the ion pump ATP4 (as mRNA and/or translated protein), changing its distribution from a symmetric to an asymmetric one (Levin et al., 2002). This asymmetry is hypothesized to generate an intracellular pH and voltage gradient, along which the small charged monoamine, serotonin, transfers via gap junctional communication (GJC) to blastomeres on the right side of the cleavage stage embryo (Fig. 1F and G; Fukumoto et al., 2005b). Almost one day later, when the embryo consists of thousands of cells, this right-sided serotonin asymmetry, by an unknown epigenetic mechanism, is proposed to repress *Nodal* activity on the right side, thereby initiating the left-asymmetric activation of the *Nodal* cascade

(Fig. 1G; Vandenberg and Levin, 2013). This mechanism for symmetry breakage will be referred to herein as the “ion-flux” model. Consistent with this model, asymmetries in serotonin, ATP4 and ATP6 were reported in early cleavage stage embryos (Adams et al., 2006; Fukumoto et al., 2005b; Levin et al., 2002). In addition, blockage of GJC or mild interference with cytoskeletal dynamics reportedly disrupts L–R development (Levin and Mercola, 1999, 1998; Lobikin et al., 2012).

When cilia-driven leftward flow was found in the neurula of the *Xenopus* embryo (Schweickert et al., 2007), as observed previously in mouse (Nonaka et al., 1998), rabbit (Okada et al., 2005), zebrafish (Essner et al., 2005) and medaka (Okada et al., 2005), the question arose as to which mechanism is principally instructive for breaking symmetry in the amphibian embryo. Advocates of the ion-flux model have suggested that, throughout the animal kingdom, symmetry breakage occurs very early, i.e. in the zygote or during the first two cell divisions, and that the function of cilia-driven fluid flow must therefore be restricted to a later-stage amplification step (Vandenberg and Levin, 2013). Here, we present our view of the conceptual problems with the ion-flux model, and evaluate the salient experimental support for each of the two opposing models. For detailed reviews on other aspects of the two models we refer to recent comprehensive reviews (Hirokawa et al., 2012; Nakamura and Hamada, 2012; Vandenberg, 2012; Vandenberg and Levin, 2013, 2010a; Yoshida and Hamada, 2014).

Embryological considerations: Spemann's organizer and left–right asymmetry

A mechanism that breaks symmetry during early cleavage stages is likely to be independent of L–R orientational cues that derive from the gastrula, or Spemann's organizer. In contrast, a mechanism that operates during or after gastrulation is likely to be strongly influenced by, or even be mandatorily dependent on, the organizer. Experimental analysis of organizer function on L–R asymmetry should thus provide an answer as to when symmetry is broken (Schweickert et al., 2012).

Spemann's and the left–right organizer: how are they related?

In frogs, symmetry breakage via cilia-driven leftward flow is intrinsically tied to Spemann's organizer. The ciliated gastrocoel roof plate (GRP), where leftward flow develops during neurulation, is derived from the superficial mesoderm (SM) of the gastrula. The SM constitutes the superficial cell layer of a region that sits above Spemann's organizer during early gastrulation (Fig. 2A and B). It is thus sandwiched between prospective neuroectoderm and the more vegetally located epithelial layer of the organizer (Shook et al., 2004). In the early gastrula, the SM expresses *foxfj1*, the main control gene for motile cilia (Stubbs et al., 2008; Fig. 2C and D). In addition, both the organizer and the central part of the GRP contain cells with eventual notochordal fate, reflecting their close relationship (Shook et al., 2004). Ciliated, flow-generating epithelia in other vertebrates, despite their common function, display a wide morphological variety (Blum et al., 2007). In this review they will be referred to as left–right organizers (LRO). In rabbit and frog, for example, the LRO develops as a flattened epithelial plate, while it appears as a concavity in the mouse, as a raised dome in medaka, and as a completely enclosed, hollow vesicle in zebrafish (Blum et al., 2009b, 2007).

We have hypothesized that the evolution of LROs and the notochord are intricately linked in the chordates (Blum et al., 2014), and it might be worthwhile to evaluate the LRO lineage in fish and mammals. In fact, embryos with defects in notochord

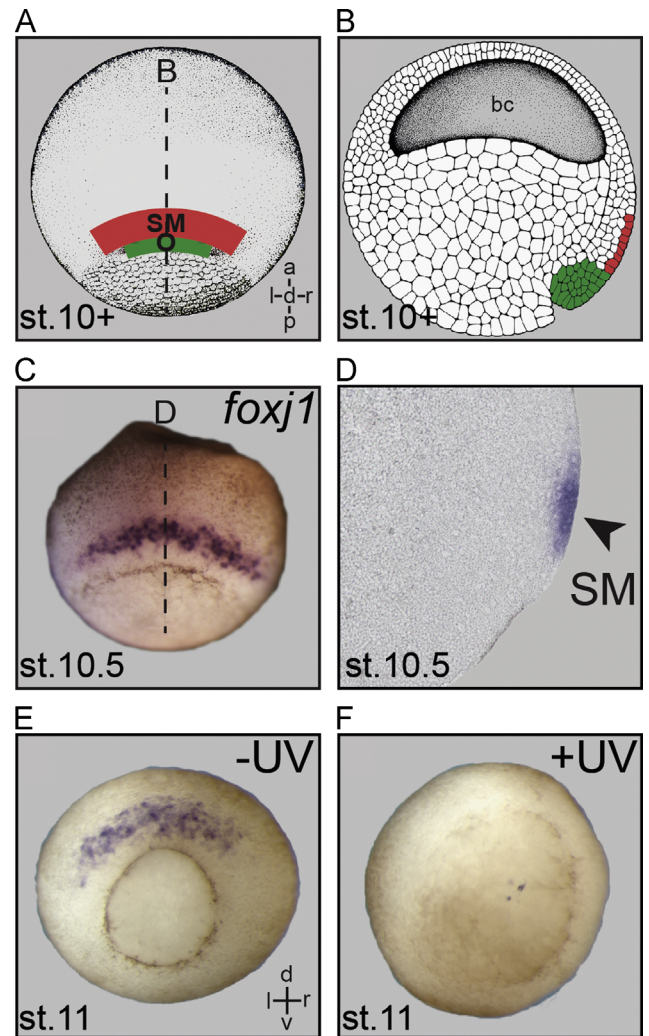


Fig. 2. Structural and functional relationship of Spemann's organizer and superficial mesoderm. (A) Schematic depiction of superficial mesoderm (SM; red) and organizer (O; green) in whole-mount stage 10⁺ gastrula embryo shown in dorsal view. (B) Arrangement of organizer and SM in a sagittal section. (C) SM *foxfj1* expression in a whole-mount gastrula embryo. (D) Sagittal section (plane indicated by dashed line in C) demonstrates *foxfj1* mRNA in the SM (arrowhead). (E and F) Loss of SM *foxfj1* expression (E) in UV-ventralized gastrula embryo (F), demonstrating the dependence of SM specification on organizer function.

formation are particularly prone to develop L–R defects: either due to defective morphogenesis of the ciliated LRO and the resultant interference with leftward flow, and/or due to absent midline barrier function of Lefty (Bisgrove et al., 1999; Cheng et al., 2000; Danos and Yost, 1996; Hamada et al., 2002; King et al., 1998; Lenhart et al., 2011; Melloy et al., 1998; see below). The classical Brachyury mouse mutant and the corresponding no tail mutation in zebrafish exemplify the relationship between LRO and notochord. In both species, this T-box transcription factor is required for notochordal integrity and development (Schulte-Merker et al., 1994; Wilkinson et al., 1990). Besides notochordal defects, brachyury (T) and no tail mutants display laterality defects (King et al., 1998). Mutant LROs are smaller and overall malformed, and ciliogenesis is strongly affected (Amack and Yost, 2004). Consequently, mutant embryos lack flow (Essner et al., 2005; our unpublished results). In *Xenopus* T (brachyury) morphant embryos, GRP development is similarly disturbed, underscoring the conserved dependence of symmetry breakage on ciliary flow (our unpublished data). These examples demonstrate that a subset of the cells comprising the organizer proper is required for L–R

development. These cells organize into an epithelial tissue, differentiate transiently into the ciliated LRO, produce the pattern-specifying leftward flow and, at least in *Xenopus*, finally contribute to the notochord (Shook et al., 2004).

Loss of organizer function invariably leads to L–R defects

The organizer is responsible for the explicit development of the embryo's overall dorso-anterior to ventro-posterior axis. Manipulation of organizer function could therefore impact not only on leftward flow, but on an additional, separate process: the midline barrier. A multitude of experiments and analyses of mutant embryos have provided compelling evidence that the midline is crucial for L–R development (Bisgrove et al., 2000; Danos and Yost, 1996; Hamada et al., 2002; Izraeli et al., 1999; Lee and Anderson, 2008; Lohr et al., 1997; Zhang et al., 2012). Besides the notochord (Lee and Anderson, 2008), the floor plate of the neural tube serves as a functional barrier; Lefty expression there prevents Nodal secreted from the left LPM from functioning on the right side (Shiratori and Hamada, 2006).

Two classical kinds of experiments in *Xenopus* have reinforced the functional connection between dorso-anterior and L–R development: (1) UV irradiation at the one-cell stage to prevent the organizer from forming in the first place (Fig. 3); and (2) mis-expression of DNA expression constructs to manipulate organizer function after it has formed following the mid-blastula transition (MBT). The vegetal outer cortex of the zygote contains determinants necessary to establish the dorsal organizer (Ku and Melton, 1993; Tao et al., 2005; Zhang and King, 1996). Normally, the vegetal cortex rotates in a microtubule-dependent manner away from the site of sperm entry, depositing these determinants on the future dorsal side, thus establishing the dorso-ventral axis (Kao and Elinson, 1988; Miller et al., 1999; Vincent et al., 1986). UV-irradiation of the vegetal cortex disrupts the microtubules needed for cortical rotation, thereby preventing dorsal accumulation of determinants and resulting in organizer-deprived, ventralized embryos (Gerhart et al., 1989). In contrast, manipulation of organizer function by dorsally targeted injection of DNA expression vectors affects the embryo after MBT, when zygotic transcription is released from repression shortly before the onset of gastrulation. Activation of the canonical Wnt pathway in the organizer territory during blastula/early gastrula stages counteracts both organizer specification and function (De Robertis et al., 2000). Although operating at different developmental stages, both treatments (the earlier UV treatment and the later Wnt pathway disruption) interfere with dorso-anterior development, because the organizer does not form or act properly. Naturally, it is not possible to observe L–R asymmetry in an embryo lacking a dorsal body axis, but it is important to ask what happens to the process of laterality specification when dorsal development has been partially disrupted. Significantly, the specification of the L–R axis appears randomized in embryos mildly ventralized by either manipulation (Danos and Yost, 1995). Thus, Spemann's organizer appears to govern not only dorsal axial but also L–R specification.

[Intriguingly, mildly ventralized tadpoles fail to form a notochord specifically in the anterior region (Danos and Yost, 1995). During gastrulation, anterior notochordal cells involute first, accompanied by the overlying SM cells (Shook et al., 2004), suggesting that the GRP is unable to form in these ventralized individuals. Indeed, the SM marker foxj1 was absent in UV-irradiated specimens (Fig. 2E and F), demonstrating that LRO specification is linked to general organizer functions.]

The concept of “early” vs. “late” induced organizers is irrelevant for L–R asymmetry

The above discussion indicates that when the endogenous organizer is damaged, laterality becomes randomized. What happens

to L–R specification when a new organizer is introduced into a fully ventralized background? Organizer reconstitution has long been a valuable tool to elucidate signaling pathways that are involved in organizer induction and specification. Two convenient methods are available in *Xenopus* embryos. First, by injecting mRNAs at the 4–32 cell stage of ventralized embryos, many factors, including components of the canonical Wnt pathway, or targets like the homeobox gene *siamois*, can completely rescue the ventralizing effects of UV by de novo organizer induction (Fig. 3; Fan and Sokol, 1997; Sokol et al., 1991). Second, mimicking the effects of cortical rotation can be used to reintroduce organizer function into irradiated embryos. Gravity-driven artificial rotation of the cortex relative to the core of the zygote after UV treatment relocates vegetal dorsal determinants asymmetrically by gravity (tipping, Fig. 3). This method effectively rescues dorso-anterior development in UV embryos (Scharf and Gerhart, 1980; Weaver and Kimelman, 2004).

Both methods, schematically summarized in Fig. 3, have been applied by proponents of the ion-flux model (Vandenberg and Levin, 2010b). The hypothesis of those experiments has been that L–R determination in cleavage-stage embryos is independent of the organizer or imprints L–R positional information onto the organizer (Vandenberg and Levin, 2010b). Because experimentally induced organizers are introduced at random positions compared to the initial primary dorsal axis, early (i.e. already fixed) L–R determinants should be mis-localized with respect to a newly introduced organizer. However, the results of these experiments do not support the hypothesis: as judged by the organ situs of tadpoles, laterality was basically restored by both tipping (95% of cases) and localized *siamois* mRNA injections (75% of specimens; Schweickert et al., 2012; Vandenberg and Levin, 2010b). Therefore, the organizer effect is dominant over any early instructive “bias”, which leads to the conclusion that the deterministic event is related to the organizer and to structures carrying instructive influence that are derived from it, i.e., the GRP/LRO.

Surprisingly, Vandenberg and Levin arrived at an unusual interpretation of their results. In short, rescues were categorized as “early” or “late” according to the presumed interval of their activity (Vandenberg and Levin, 2010b). As the transcription factor Siamois is only able to activate organizer target genes after MBT it was coined a “late induced organizer”, while tipping of the zygote was referred to as an “early induced organizer” (Vandenberg and Levin, 2010b). The slightly lower rescue efficiency of *siamois* was taken as supporting the view that “late induced organizers” lack early L–R cues, implying that they must be present in the “early induced organizer”. This interpretation is insupportable for (at least) three reasons. First, it is problematic to compare two completely different methods, an invasive (injection) to a non-invasive one (tipping; Fig. 3). We are not aware of any injection experiment that results in one hundred percent efficiency of rescue – it is a technical fact of life that the intracellular distribution of an injected RNA can only approximate that of the endogenous transcript. In addition, because mildly UV-ventralized embryos are profoundly impaired for laterality specification (Fig. 3F; Danos and Yost, 1995; Lohr et al., 1997), the rescue of 75% wild-type organ situs in *siamois*-injected UV-treated embryos (Vandenberg and Levin, 2010b) appears very high. Researchers familiar with rescue of morpholino oligonucleotide-mediated gene knockdowns in most cases have to live with lower (yet significant) rescue efficiencies. It would be interesting to know whether the organizer function was fully rescued in all cases, i.e. whether specimens with heterotaxia had normal heads and body axes. Unfortunately, this important information was not reported (Vandenberg and Levin, 2010b). Second, the result of the *siamois* rescue is not in accordance with the authors' own hypothesis, which predicts a loss of laterality upon loss of the early asymmetric cues in UV irradiated embryos. Vandenberg and Levin (2010b) scored three asymmetric organs of

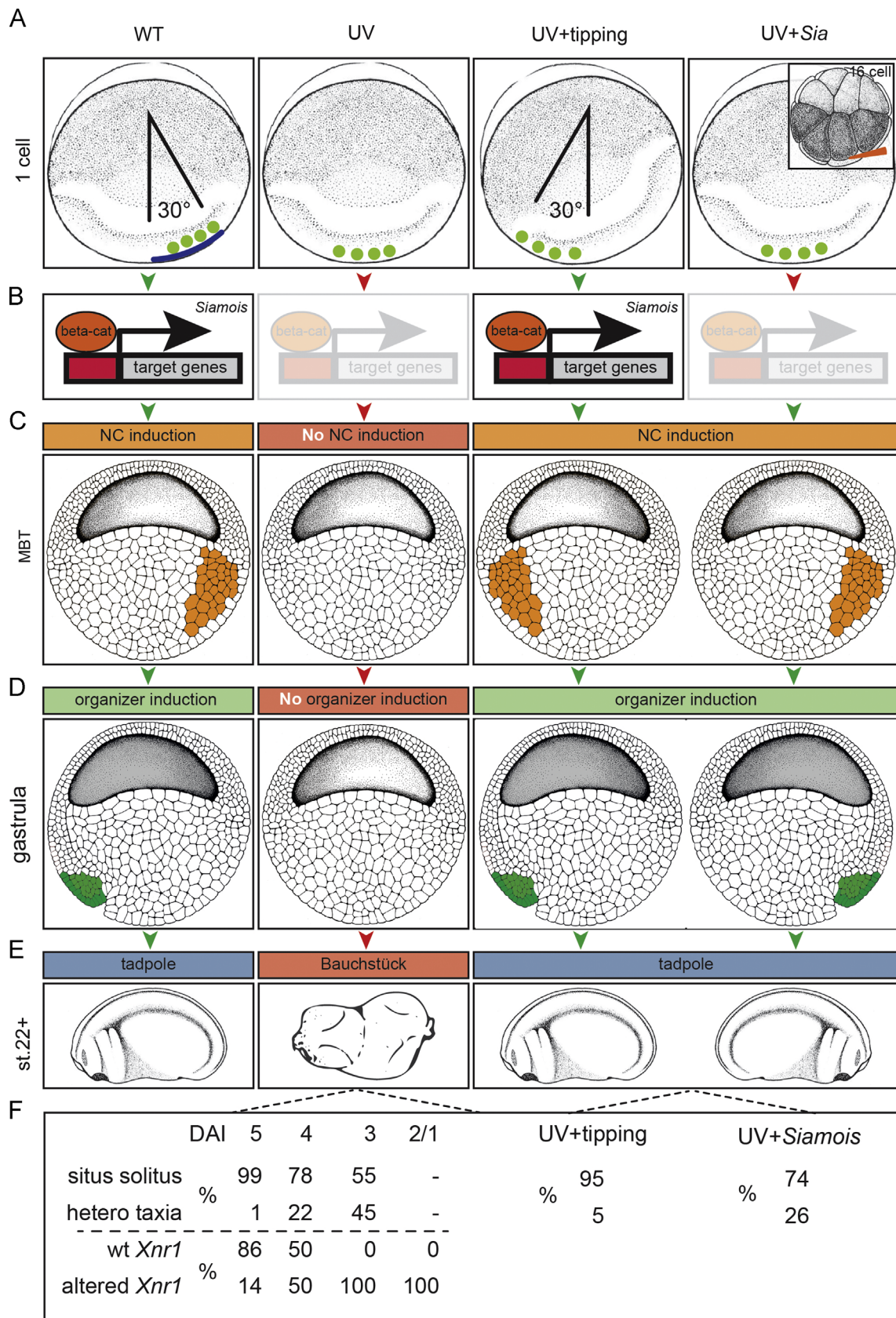


Fig. 3. Laterality in UV-treated and rescued embryos. In wildtype (WT) embryos, cortical rotation (blue line) relocates determinants (green circles) to the future dorsal pole (A). Wnt/ β -catenin dependent transcription of *siamois* (B) induces the Nieuwkoop Center (NC; C, orange), following the onset of zygotic transcription at the mid-blastula transition (MBT). The NC induces the formation of the gastrula organizer and SM (D, green), resulting in tadpoles with normal laterality specification (E). UV-irradiation of the zygote inhibits cortical rotation and prevents relocation of determinants (green) to the future dorsal pole. Lack of NC and organizer induction results in ventralized embryos (“Bauchstück” or belly piece of dorso-anterior index: DAI=0) without discernible organs or organ situs. (F) Depending on the degree of UV-induced ventralization, graded responses were observed, both with respect to organ situs (Danos and Yost, 1995) as well as left-asymmetric *Xnr1* expression in the LPM (Lohr et al., 1997). Manual tipping of UV-irradiated specimens relocates determinants, induces NC, *Siamois*, organizer and SM function and thus rescues laterality, as does *Siamois* mRNA injection into vegetal blastomeres at random positions of the 16-cell embryo (Vandenberg and Levin, 2010b).

the frog tadpole, heart, gut and gall bladder. As each organ can individually adopt a wild type or reversed orientation, the maximal theoretical percentage of situs solitus in batches of embryos showing a completely random assortment of these independent organ locations should be 12.5% (Fukumoto et al., 2005b), close to the value observed in UV embryos when scored for Nodal cascade induction. Situs solitus in three out of four *siamois*-injected UV embryos thus rather reflects an efficient restoration of laterality than a loss of L–R identity. Third, the idea that leftward flow amplifies early L–R cues does not help the argument – if cues are gone, what is available to be amplified? Vandenberg and Levin (2010b) reported high efficiencies of UV-treatments, affecting 94–97% of specimens in any given experiment. If L–R cues were that effectively destroyed, what could leftward flow amplify in *siamois*-induced “late” organizer specimens?

We therefore contend that the organizer's activity as a vectorial instructor of laterality does not require any preceding cues for its activity. In normal embryos, factors absolutely restricted to early cleavage stages of activity have not been identified, and there is no strong requirement for such cues in order to yield L–R asymmetry. But even if hypothetical early determinants were to be aligned with the organizer's vector of action, the requirement for these determinants needs to be experimentally shown. We conclude from these lines of arguments that setting up the L–R axis is an intrinsic feature of the organizer, a notion initially put forward almost 20 years ago (Nascone and Mercola, 1997). The laterality program is not executed unless the organizer is functioning, and it emerges de novo from the activity of the organizer or tissues that are readily derived from it.

Nodal cascade induction in the LPM depends on flow

One additional point of embryological reasoning must be addressed here, which has been used to suggest that Nodal cascade induction occurs prior to cilia-dependent flow. Because the ion-flux model assumes a constitutive early induction of the Nodal cascade in the LPM on both sides of the neurula stage embryo, Levin et al. used LPM explants to test whether Nodal induction is independent of leftward flow. They isolated left LPM explants of embryos at stages 13, 18 or 22, i.e. before, during and after leftward flow. Because activation of Nodal cascade genes was later detected in “the vast majority of explants” (Vandenberg et al., 2013a), it was argued that a cilia-dependent induction of Nodal expression in the left LPM could not have occurred in stage 13 explants. We do not subscribe to these conclusions and herewith provide a robust alternative explanation. As previously reported (Lohr et al., 1997), at least some isolated LPM explants indeed have the ability to activate the Nodal gene cascade at stages 23 and 24. However, we know that this phenomenon is highly sensitive to a microsurgically introduced experimental variable – precisely where the explant is made, relative to Nodal's primary secretion site at the posterior midline, the lateral cells of the LRO (Ohi and Wright, 2007). In addition, L–R asymmetry is highly sensitive to, and dependent upon, dynamic interactions between the left and right sides, which of course can only be true in intact and undisturbed embryos.

Both sides seem to be completely competent to activate Nodal expression initially. The asymmetry comes from the specification of the left side as having a small advantage over the right side, and the necessity to work continually to suppress the activation of the Nodal auto-regulatory loop on the right side. Indeed, right-sided expression of Nodal, even in whole normal embryos, is detected at low levels, while the targets *Lefty* and *Pitx2* are not (Ohi and Wright, 2007; our unpublished qRT-PCR results). Therefore, explantation needs to take into account the loss of the suppressive

influence from the left side, and especially the timing of the explantation. In our own hands, explants varying by “only a stage or so” (i.e., a few hours) can produce dramatically different effects. Moreover, the in situ hybridization detection method requires real attention to detail with certain probes that are subject to “background artifacts”, and Nodal is one of these – especially in frog embryos.

Since Nodal stimulates its own expression, early explants that happen to contain the very posterior paraxial part of the embryo, directly adjacent to the zone of bilateral Nodal expression, would subsequently be able to auto-activate Nodal in the LPM at stage 24. In contrast, precisely cut early explants, only comprised of central parts of the LPM, and clearly free of posterior-most structures, do not activate Nodal (Ohi and Wright, 2007). Importantly, the same kind of explants in post-flow stages express Nodal perfectly (on in left-side explants, off in right-side ones). The most plausible explanation for the left-sided induction of Nodal in explants excised in early, pre-flow stages is that these stage 13 explants must have included parts of the tissue that in later stages comprises the bilateral Nodal domain (or that this type of tissue arises post-explantation by a regulative process), and therefore autonomously secretes Nodal. A close look at the published stage 24 specimen, which was explanted at stage 13, endorses this notion, as this embryo clearly has head structures and a cement gland, indicating imperfect preparation of at least this specimen (Fig. 1D in Vandenberg et al., 2013a). Several additional points critiquing the conclusions of Vandenberg and Levin (2013) are reserved for the specialist reader in a Supporting information. In summary, we state that asymmetric LPM Nodal cascade induction strictly depends on the physical presence of Spemann's organizer and cilia-driven leftward flow. Following these embryological considerations, we now turn to a discussion of asymmetrically expressed factors and their relationship to L–R axis formation.

Asymmetric expression of mRNAs and proteins during embryonic development

Most species with an asymmetric body plan, with the marked exception of ecdysozoa, express the Nodal cascade asymmetrically. This is true for snails (Grande and Patel, 2009; Vandenberg and Levin, 2013), as representatives of the protostomes, as well as for all deuterostomes, including primitive chordates (amphioxus and *Ciona*) and the vertebrates (Blum et al., 2014; Chea et al., 2005). In deuterostomes, Nodal is exclusively found on the left side. A potential exception to this general pattern was presented by the sea urchin pluteus larva, in which expression was described as right-sided (Molina et al., 2013). However, this may not necessarily reflect a discrepancy, but rather how the pluteus body axes are mapped onto the more familiar vertebrate body plan. The alignment of the D–V axis of the larva conventionally follows the oral–aboral polarity, i.e. placing the mouth on the ventral side. However, because the oral ectoderm expresses typical dorsal organizer genes such as *chordin* and *gooseoid* (Li et al., 2013, 2012), the older convention should be functionally inverted, and thus the mouth of the larva more properly represents the dorsal pole of the embryo (Blum et al., 2014, 2009b). With this topological reassignment, the pluteus larva's left and right sides are reversed and, relative to the organizer, the Nodal cascade is expressed in a left-asymmetric manner, consistent with all other higher organisms investigated so far.

Embryos using leftward flow during early neurulation display a second consistent molecular asymmetry. This asymmetry precedes induction of the Nodal cascade in the LPM. It is found in cells bordering the LRO on both the left and right side and relates to the

Table 1
Reported asymmetries of presumed early acting L–R determinants.

Factor	Detection	Stage	Site	Frequency	References
Serotonin		IHC 32–64 Cells	Right ventral	8/8 Consensus (n=10) n. sp.	Vandenberg et al. (2013a) Fukumoto et al. (2005b) Adams et al. (2006)
Serotonin		IF 32–256 Cells	Symmetrical	100% n > 200	Beyer et al. (2012a)
atp4 alpha	mRNA	ISH 2–4 Cells	Right-sided	n. sp.	Aw et al. (2008)
atp4 alpha	mRNA	ISH 2 Cell-blastula	Symmetrical	100% n=320	Levin et al. (2002)
atp4 alpha	Protein	IHC 2 Cells	Right	n. sp.	Walentek et al. (2012)
atp4 alpha	Protein	IHC 4 Cells	Right ventral	n. sp.	Aw et al. (2008)
atp4 beta	Protein	IHC 2–4 Cells	Right (do+ve)	n. sp.	Aw et al. (2010)
atp4 alpha	Protein	IF 4 Cells	Right (do+ve)	n. sp.	Aw et al. (2008)
atp6v0a2	mRNA	ISH 4 Cells	Symmetrical	n. sp.	Rutenberg et al., 2002
atp6v0c	Protein	IHC 2–8 Cells	Right (do+ve)	> 80%	Adams et al. (2006)
Atp6v1a/b/f				n. sp.	
atp6v0c/ductin	Protein	IHC 4 Cells	Right ventral Left dorsal	55% 11% n=110	Vandenberg et al. (2013b)
KCNQ1	Protein	IHC 2 Cells	Right	n. sp.	Morokuma et al. (2008)
KCNQ1	Protein	IHC 4 Cells	Right ventral	n. sp.	
KCNQ1	Protein	IHC 4 Cells	Right ventral Dorsal left Symmetrical	34% 18% 27% n=85	Vandenberg et al. (2013b)
KCNE1	Protein	IHC 2 Cells	Left	n. sp.	Morokuma et al. (2008)
dnah11	Protein	IHC 4 Cells	Left or right ventral	n. sp.	
dnah11	Protein	IHC 2–8 Cells	n. sp.	n. sp.	Qiu et al. (2005)
KIF3B	Protein	IHC 2 Cells	n. sp.	n. sp.	Qiu et al. (2005)
Polaris	Protein	IHC 4 Cells	Absent in one right blastomere	n. sp.	
Polaris	Protein	IHC 2 Cells	n. sp.	n. sp.	Qiu et al. (2005)
Polaris	Protein	IHC 4 Cells	Symmetric	n. sp.	
Inversin	Protein	IHC 4–8 Cells	Right > left	n. sp.	Qiu et al. (2005)
ac. tubulin	Protein	IHC 2–4 Cells	Left (do+ve)	n. sp.	Qiu et al. (2005)
Detyrosinated tubulin	Protein	IHC 4 Cells	Left (do+ve)	n. sp.	Qiu et al. (2005)
14-3-3E	Protein+mRNA	ISH IHC 2–4 Cells	Right (do+ve)	n. sp.	Bunney et al. (2003)
Dvl2	Protein	IF 4 Cells	Right-ve in animal-vegetal Sections symmetrical in transversal sections	8/9 14/14	Vandenberg and Levin (2012)

Studies which failed to reproduce early serotonin and ATP4 L–R asymmetries are highlighted in gray shade. do, dorsal; ve, ventral; n.sp., not specified.

dand5 gene which encodes an inhibitor of Nodal. It is known by different names – *Coco* in *Xenopus*, *charon* in fish and *Dante/Cerl2* in mammals (Hojo et al., 2007; Marques et al., 2004; Vonica and Brivanlou, 2007). In all these organisms, *dand5* is co-expressed with Nodal during early neurula stages. However, as a consequence of leftward flow, *dand5* mRNA expression becomes down-regulated on the left side, resulting in a right-asymmetric expression pattern. Down-regulation of *dand5* has been shown to be essential for the subsequent induction of the Nodal cascade in the left LPM (Hojo et al., 2007; Nakamura et al., 2012; Schweickert et al., 2010; Fig. 1C–E).

Further asymmetries in gene expression have been reported for chick and *Xenopus* embryos. In the chick, asymmetries have been observed at gastrula stages (Levin, 2005; Levin et al., 1995; Raya and Izpisua-Belmonte, 2004). Most of these result from the above-mentioned chiral (left-sided) cell migration at Hensen's node. Mechanical or pharmacological interference with node rotation prevents establishment of these asymmetries, i.e. they are the result and not the cause of symmetry breakage in the chick (Gros et al., 2009). In *Xenopus*, in contrast, a large inventory of molecular asymmetries has been reported during early cleavage stages, many of which have been integrated into different versions of the ion-flux model (Fig. 1F and G; Table 1). These can be grouped into ion channels (ATP4, ATP6, KCNQ1, KCNE1), motor proteins (Dnah11, KIF3B), cytoskeletal components (acetylated and detyrosinated tubulin) and others (serotonin, 14-3-3E, disheveled-2/dvl2, inversin, IFT88/polaris). In a recent review, the advocates of the ion-flux

model remarked that “molecular evidence for early models in mammalian model systems remains one of the major unaddressed opportunities in this field” (Vandenberg and Levin, 2013). Actually, we have in the past quite rigorously analyzed the possibility of pH and voltage gradients, i.e. the basis of the ion-flux model. To wit, we made very careful measurements to detect potential pH and voltage gradients across the large, flat, and easily imaged rabbit blastodisc. Our thorough investigations of embryos of different stages using the pH-sensitive fluorescent dye BCECF-AM failed to detect consistent imbalances between left and right sides (Feistel, 2007).

The early-asymmetry model in its current version (or “iteration”) requires the asymmetric localization of two crucial components (Fig. 1F): (1) ATP4, as mRNA or protein, has to localize asymmetrically to the ventral right lineages before the first cleavages partition the zygote's cytoplasm; (2) serotonin has to be driven through functional gap junctions to “pile up” in a single early ventral-right blastomere by the 32–64 cell stages. To test this model directly, we carried out some basic descriptive investigations for serotonin and ATP4.

ATP4

ATP4 was found in the animal hemisphere of embryos from the zygote throughout late cleavage stages. L–R differences were never encountered (Walentek et al., 2012). In a publication subsequent to the original description Levin and colleagues reported “significant variability of in situ signal in embryos from different females” (Aw et al., 2008). We therefore analyzed hundreds of embryos from

different females from our own frog colony and from a separate colony of a colleague, but still did not find a single embryo with L–R asymmetric *ATP4* expression (Table 1; Walentek et al., 2012). Of course, we cannot exclude that asymmetries occur in very rare cases. It seems inescapable that infrequent events cannot qualify as the basis for robust laterality formation in the amphibian embryo.

Serotonin

Serotonin asymmetry should be easily detectable, but it is not. We initially became interested in the ion-flux hypothesis because an immunocytochemically assayed lineage-specific enrichment of serotonin (as reported by Fukumoto et al., 2005b) would have been an extremely useful readout for studying experimental perturbations of early localization mechanisms (Danilchik et al., 2006). Disappointingly, and following considerable effort, we were never able to demonstrate a consistent enrichment of endogenous serotonin (Beyer et al., 2012a). Further, microinjected serotonin, easily detected by whole-mount immunocytochemistry, failed to relocate to uninjected blastomeres (Beyer et al., 2012a), demonstrating that it rapidly becomes sequestered into some bound form (e.g. vesicles), which cannot pass through gap junctions (cf. Fig. 4, below). Thus, we are forced to question both the early localization of an electrogenic maternal factor (such as ATP4) as well as the directed passage of serotonin through gap junctions. A third, little-discussed possibility, that serotonin might be selectively degraded in some particular lineage, also must be discounted, since exogenous serotonin observably persists in any lineage into which it is microinjected (Beyer et al., 2012a).

Previously published reports of maternal asymmetric localizations

Unfortunately, it is difficult to develop a comprehensive picture from published reports – in most cases the numbers of analyzed specimens and frequencies of observed asymmetries were not reported (Table 1). For three particular factors, numerical data are available – right-side asymmetries were reported for *KCNQ1* in 34% of cases (Morokuma et al., 2008), for the ductin subunit of ATP6 in 55% of analyzed specimens (Vandenberg et al., 2013b), as well as in 8/9 embryos analyzed for *Disheveled-2* (*Dvl2*) expression (Vandenberg and Levin, 2012; Table 1). With the exception of *Dvl2*, these rates are too low to explain the normally robust (>95%) expression of situs solitus in undisturbed *Xenopus* embryos. The *Dvl2* data set, aside from the low number of analyzed embryos, suffers from another complication. In Vandenberg and Levin (2012) two planes of sections of *Dvl2*-analyzed specimens are shown. Along the animal–vegetal axis, *Dvl2* protein immunodetection showed uniform expression in the animal hemisphere of the 4-cell embryo, i.e. both cells of the section contain protein. This reportedly was observed in 14/14 cases. In transverse sections, in contrast, right asymmetries were reported to occur in 8/9 cases. Only one pattern can be correct – if *Dvl2* is found in both cells in sections along the animal–vegetal axis, transverse sections at the level of staining in the animal half of the embryo should show all four cells positive for *Dvl2*. Or, conversely, a consistent ventral–right asymmetry in transverse sections would mean that specimens sectioned along the animal–vegetal axis would also reveal this clearly asymmetric pattern. The published results on *Dvl2* protein expression need to be carefully reconsidered as potentially misinterpreted from a slightly oblique plane of section relative to the transition between *Dvl2*-containing and *Dvl2*-lacking regions along the animal–vegetal axis. Clearly, whole-mount type analyses, marked carefully with respect to the dorso–ventral axis, could negate this criticism. In summary, there is presently no

compelling evidence for consistent cleavage-stage asymmetries in maternal factors with causal roles in L–R determination.

Taken together, the available data on asymmetric expression of mRNAs and proteins support, rather than discount, the pivotal roles of the Nodal cascade and, in the case of leftward flow, of the Nodal inhibitor *dand5* for laterality determination. Other, presumably early-acting factors including *Dvl2* might of course be involved in the different steps of laterality determination, which has been shown for quite a number of them in the past (see below). It is not necessary, however, that such factors are asymmetrically expressed, in particular if they are involved in the specification or morphogenesis of the symmetrical LRO.

Genetic evidence supports cilia-based laterality determination in the vertebrates

There is overwhelming genetic evidence that malformation of cilia structure and function causes laterality defects in fish, mouse and humans. Many excellent reviews have covered this topic (Biggrove et al., 2003; McGrath and Brueckner, 2003; Norris and Grimes, 2012; Oh and Katsanis, 2012; Shiraishi and Ichikawa, 2012; Sutherland and Ware, 2009). Human ciliopathies, i.e. syndromes characterized by ciliary malfunctions, frequently display laterality defects. The first laterality syndrome, caused by immotile cilia, was Kartagener syndrome, in which patients show defects in the ciliary motor protein *Dnah11* (formerly known as left–right dynein, *lrd*; (McGrath and Brueckner, 2003)). Kartagener syndrome belongs to the larger group of primary ciliary dyskinesia (PCD) syndromes. Other ciliopathies with left–right defects involve, among others, polycystic kidney disease, Bardet–Biedel syndrome, Meckel–Gruber syndrome, Joubert syndrome and nephronophthisis (Norris and Grimes, 2012).

Various genetic screens in mouse and zebrafish underscore the importance of cilia for L–R axis formation. Dominic Norris (Harwell) performed an ENU-based screen for L–R patterning defects in mouse and identified mostly cilia-related genes (Ermakov et al., 2009; Field et al., 2011). Cecilia Lo (Pittsburgh), in a recessive screen for congenital heart disease, scanned >65,000 fetuses by ultrasound in utero, identified >3000 abnormal embryos and established 192 lines. Of the 69 laterality-defective individual mouse lines derived, 82% showed mutations in cilia-related genes (Liu et al., 2013; Cecilia Lo, personal communication). Finally, knockouts of genes encoding intraflagellar transport proteins (IFT), motor proteins (dyneins and kinesins) or transcription factors involved in ciliogenesis (i.e. *foxj1*, *Rfx*) inevitably resulted in laterality defects (for a recent review see Yoshida and Hamada, 2014). In zebrafish, general L–R screens are difficult to perform because of the very high rates of background laterality defects in non-isogenic lines, which can be as high as 10–15% (Rebecca Burdine, Princeton, personal communication), possibly related to some subtle but fairly pervasive environmental disturbance. Still, re-screening of the Tübingen collection for L–R patterning defects in the heart uncovered primarily cilia genes (Chen et al., 2001; Panizzi et al., 2012; Schottenfeld et al., 2007; Serluca et al., 2009; Sullivan-Brown et al., 2008). In addition, a genetic screen for cystic kidneys identified cilia genes, and many of the mutants display L–R defects as well (Sun et al., 2004). These genetic screens certainly cement the importance of cilia in laterality determination.

As mentioned above, it has been proposed that cilia-driven leftward flow merely acts as an amplification step for asymmetry that is initially defined by ion-flux during early cleavage (Vandenberg and Levin, 2013). This proposal predicts that asymmetry defined by ion-flux should be present in the absence of flow, unless it is mandatorily gated through the cilia/LRO machine.

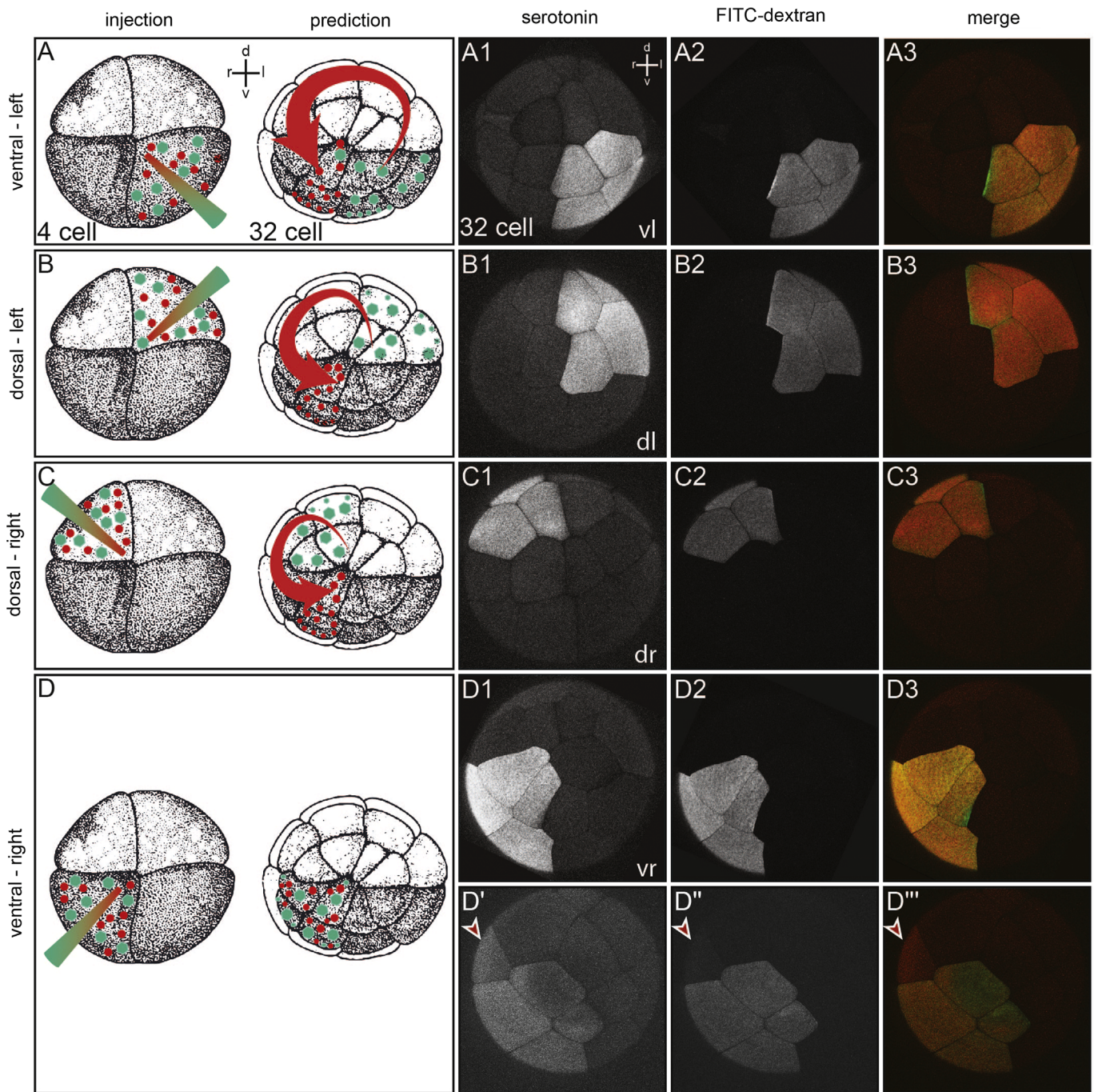


Fig. 4. Serotonin fails to relocate according to the ion-flux model's prediction. Embryos were selected that displayed regular and symmetric cleavage patterns relative to the pigmentation differences established by the sperm entry point. (A–D) Experimental design (injection) and prediction. A mixture of serotonin and fixable fluorescein dextran (FITC) was microinjected into ventral-left, dorsal-left, dorsal-right, or ventral-right quadrants of 4-cell embryos, respectively. According to the ion-flux model (prediction), serotonin (red) should translocate counterclockwise from the site of injection and accumulate in the ventral right quadrant, while the fluorescein-dextran (green) should remain in situ. (A1–D3) Embryos were fixed at the 32-cell stage and examined via whole mount confocal microscopy to detect potential redistribution of serotonin (A1–D1) relative to the fluorescein dextran (A2–D2). Enrichment of serotonin in the ventral-right lineage was not observed (merged images; A3–D3). (D'–D''') Displacement of serotonin into uninjected lineage is frequently accompanied by lineage label (cf. Table 3). (D'–D''') In the individual case of a ventral-right injection shown here, serotonin has leaked across the second cleavage plane into the dorsal-right quadrant (D'', arrowhead). The same blastomere also received small amounts of fluorescent dextran (D''', arrowhead), revealing the existence of a persistent cytoplasmic bridge between the dorsal and ventral lineages (cf. Fig. 5).

Two lines of experimentation have addressed that question. The first approach manually ablated the ciliated epithelium or the precursor tissue, respectively. When Kupffer's vesicle was mechanically destroyed in Medaka fish (*Oryzias latipes*), massive laterality defects occurred (Bajoghli et al., 2007). Removal of the SM in the gastrula *Xenopus* embryo (Blum et al., 2009a), or laser ablations of dorsal forerunner cells in zebrafish (Essner et al.,

2005), from which the ciliated LROs (GRP and KV) develop during early neurulation, resulted in the same outcome. Remarkably, in all cases no other morphological defects arose besides disruption of laterality (Bajoghli et al., 2007; Blum et al., 2009a; Essner et al., 2005). The second type of experiment interfered with flow directly, without manipulation of tissues, cilia or genes involved in setting up flow. Methylcellulose was applied to the ciliated

epithelia in cultured frog (Schweickert et al., 2007) and mouse (Nakamura et al., 2012) embryos to hamper fluid transport by increasing the viscosity of the medium. These manipulations prevented the induction of the Nodal cascade in a high and statistically significant percentage of cases.

[The fact that procedures to ablate flow do not reach one hundred percent efficiency is intrinsic to all experimental manipulations of embryos and can be readily explained. The time point of treatment in some cases might have been too late, after fixation of laterality cues. Targeting of methylcellulose to the ciliated LRO is challenging in frog, as it has to be applied blindly directly into the gastrocoel. In the great majority of cases in which procedures did work, however, potentially early-acting ion-flux based mechanisms would have been active, and thus would have left a mark of asymmetry in every single case. Since such an outcome was not observed in all of these experiments, early ion-flux cannot be invoked as the responsible mechanism].

In summary, experimental LRO manipulations together with human, mouse and zebrafish genetics seem to indicate beyond reasonable doubt that motile cilia are required for the formation of situs solitus, and do not act by amplifying some earlier deterministic laterality signal.

Role of serotonin, ATP4 and GJC in laterality specification

In the light of these genetic data, what role might “early” determinants play in the process of laterality specification? A large body of published results from one laboratory, mostly involving pharmacological manipulation in early frog embryos, suggests involvement of maternal factors in L–R axis formation (reviewed in Vandenberg and Levin, 2013). It has been suggested that some of these factors, such as motor proteins, act during early cleavage stages prior to formation of any cilia. The implication is therefore that ciliary proteins must be carrying out laterality-specifying functions in the cytoplasm (Vandenberg and Levin, 2013). Indeed, the ion-flux model requires that motor proteins move mRNAs and proteins to the ventral-right blastomere in the early cleavage-stage embryo. In *Xenopus*, often huge amounts of many mRNAs and proteins of maternal origin are present in the zygote. However, in no single case have the consequences of pharmacological manipulations of “early” factors on flow-related processes been analyzed. After the discovery of the frog LRO and flow (Schweickert et al., 2007), we wondered whether early determinants and leftward flow acted sequentially or in parallel, and chose to analyze the central components of the ion-flux model, ATP4, serotonin and GJC in the context of flow. In the following, we briefly summarize results of these recently published studies.

Serotonin signaling

Flow and asymmetry were lost in embryos in which serotonin signaling was down-regulated (Beyer et al., 2012a). Importantly,

we found that serotonin accumulated in the epithelial cell layer of the blastula from the 128-cell stage onwards, i.e. in the same layer where the SM forms on the dorsal side (Beyer et al., 2012a). Molecularly, the SM, from which the LRO derives in the frog, is characterized by the expression of *nodal3* and *foxj1*. Both genes were down-regulated upon loss of serotonin signaling. *Nodal3* induction depends on canonical Wnt signaling. We showed that serotonin acts as a competence factor for canonical Wnt signaling, i.e. that the role of serotonin in L–R axis formation lies in the Wnt-dependent specification of the superficial mesoderm (Beyer et al., 2012a).

ATP4

Gene knock-down or pharmacological inhibition of ATP4 compromised organ situs, asymmetric gene expression and leftward flow. The GRP analysis revealed fewer, shortened and misaligned cilia. *Foxj1* was down-regulated in the SM. ATP4 was required during consecutive steps of L–R axis formation – for Wnt/ β -catenin regulated *Foxj1* induction in the SM and for Wnt/PCP dependent cilia polarization in the GRP (Walentek et al., 2012). In summary, our work on serotonin and ATP4 defines a new SM/GRP/Flow (SGF) module for symmetry breakage in frogs (Table 2). This module spans the time period from late blastula/early gastrula (SM specification) to the flow-dependent down-regulation of the Nodal inhibitor *Coco* at the left margin of the GRP at stage 19, which is the first molecular asymmetry and instrumental for Nodal cascade induction in the left LPM (Schweickert et al., 2010).

GJC and serotonin localization

We and others recently showed that GJC is required later in development for the transfer of asymmetric cue(s) from the midline to the lateral plate mesoderm in frog and mouse (Beyer et al., 2012b; Viotti et al., 2012). In the frog, *connexin26* expression in the endoderm between the LRO/GRP and the LPM is required for Nodal cascade induction downstream of flow. Inhibitor experiments in addition strongly argue against earlier functions of GJC in laterality determination (Beyer et al., 2012b). However, it remains a formal possibility that GJC also acts much earlier in development, i.e., during the first few cleavage divisions. Indeed, the ion-flux model requires that GJC exists between nearly all of the early blastomeres, except those along the incipient ventral midline.

Because early blastomeres begin a new cleavage furrow before having fully completed the preceding round of cytokinesis, it has been experimentally difficult, using small-molecule lineage tracers, to demonstrate authentic GJC against the background of open cytoplasmic bridges. Thus, the degree of physiological coupling of blastomeres via gap junctions in the earliest cleavage stages has remained controversial (Guthrie, 1984; Landesman et al., 2000). To revisit GJC in the context of a potential early localization of serotonin, we microinjected single blastomeres at the late 4-cell stage with a mixture of serotonin and a fixable fluorescent

Table 2
Module of L–R development. Timing of developmental stages and L–R modules.

Stage h	St. 1–3 0–2 h 1–4 Cells	St. 6–9 3–7 h Blastula	St. 10–14 9–20 h Gastrula–early neurula	St. 15–18 17–20 h Neurula	St. 19–45 20–106 h Tadpole
LR module	“Ion-flux”	Serotonin localization	SGF	Flow	Nodal cascade and organ situs
Readout	Nodal cascade and organ situs	SGF	SM Xnr3 Foxj1	GRP Ciliation Morphology Marker genes	Quality Directionality Coco

Table 3
Coupling of blastomeres in the 4-cell *Xenopus* embryo.

	DR-DL	DL-DR	DL-VL	VL-DL	VL-VR	VR-VL	VR-DR	DR-VR
Coupled	5	6	7	6	2	3	8	5
Not coupled	2	3	5	3	10	8	3	2
% Coupled	0.71	0.67	0.58	0.67	0.17 ^a	0.27 ^a	0.73	0.71

Compilation of results from serotonin-FITC injection experiments (cf. Fig. 4). D, dorsal; L, left; R, right; V, ventral.

^a Low transfer rates between ventral left and right blastomeres, consistent with a lack of cytoplasmic bridges (cf. Fig. 5).

dextran. Embryos were fixed at the 32-cell stage, processed for whole-mount immunocytochemistry, and examined via confocal microscopy to determine the extent to which exogenous serotonin can move across cleavage planes independent of the larger molecular weight dextran (Fig. 4). We reasoned that, if the low-molecular weight serotonin utilizes GJC to diffuse from an injected lineage, it should partition entirely free from the higher molecular weight dextran, since the latter can only move from lineage to lineage through persistently open cytoplasmic bridges.

In the vast majority of injected embryos, as shown with representative samples for each injected lineage (Fig. 4; numbers in Table 3), both serotonin and fluorescent dextran remained confined exclusively to the lineage derived from the injected cell. Upon close inspection, however, a small amount of serotonin was frequently detected in adjacent uninjected lineages. In most such embryos (29 of 39 cases; > 74%), serotonin was accompanied by faintly detectable signal from the large fluorescent dextran (Fig. 4), indicating the presence of open cytoplasmic bridges through which both injected compounds must have transferred. As shown in Table 3, this bridge-dependent exchange between injected lineages is not completely random – while exchange was observed in 58–73% of injected lineages between dorsal, left and right quadrants, only 17–27% of labeled lineages exchanged injectates across the ventral midline, i.e. between ventral-left and -right lineages.

We draw three conclusions from this result: (1) serotonin becomes rapidly bound or sequestered following its injection into the cytosol, limiting its diffusion, even though open cytoplasmic bridges remain; (2) there is no compelling evidence for gap-junctional passage of serotonin between blastomeres; (3) less exchange occurs across the ventral midline than elsewhere because there is likely no cytoplasmic bridge between ventral lineages – this bridge finishes closing on the dorsal side of the embryo (Fig. 5).

Hypothesis: “early” determinants act in the context of flow

Two main conclusions emerge from studying early determinants in the context of flow: (1) the SM plays a central role at early stages of L–R axis determination; (2) serotonin, ATP4 and GJC act in the context of flow, strongly countering the “ion-flux” model in its present form. We hypothesize that all “early” factors impinge on the SM/GRP/Flow module (cf. Table 2) for the following reasons: (1) the concept of “early” determinants (Levin et al., 2002) were developed from relatively late stage readouts of the effects of early experimental manipulations (Table 2). The efficiencies of drugs in perturbing L–R specification were generally low (Tables 4 and S1–S4). Since many drugs also affect dorso-anterior development, doses had to be carefully titrated to avoid toxicity, and to allow sufficient dorso-anterior development that laterality could even be assessed (Vandenberg and Levin, 2012); (2) importantly, more than 10 years after the original proposal of “ion-flux” based symmetry breakage, no testable model has emerged that connects putative cleavage-stage asymmetries to the left-sided

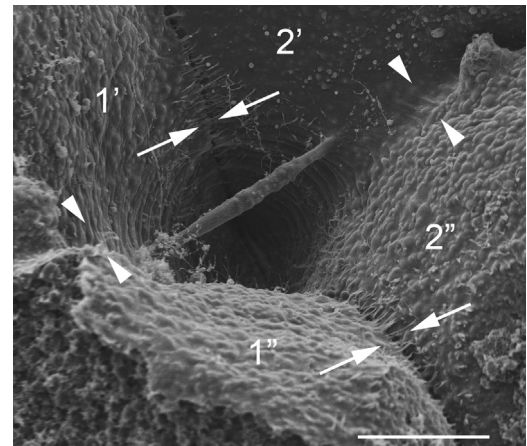


Fig. 5. Cytoplasmic bridges maintain continuity between subsets of sister blastomeres. Shown is the blastocoel-facing surface of four sister blastomeres of an embryo fixed at the onset of the 5th cleavage (16–32 cell stage), with two cleavage furrows indicated. An older, nearly-complete furrow (arrows), produces sister blastomeres 1 and 2. The nearly-closed cytoplasmic bridge remains in the form of a midbody suspended between 1 and 2 across the blastocoel. With the next cleavage cycle, a later cleavage furrow (arrowheads), separates 1' from 1'' and 2' from 2''. It is evident that 1'' and 2'' will become topologically isolated from each other, while cytoplasmic continuity can persist between 1' and 2' as long as the cytoplasmic bridge remains.

Nodal cascade at neurula stages. Experimentally, the burden remains on this hypothesis that early manipulations do not simply damage the relevant tissue's morphological pattern or signaling capacity; (3) manipulation of Coco by gene knockdown induces the Nodal cascade in the right LPM with > 80% efficiency (reaching 100% in isolated experiments; Tables 4 and S5). Coco down-regulation represents an immediate effect of flow (Fig. 1A–E), demonstrating that flow is the decisive step in laterality determination in the frog (Schweickert et al., 2010).

On the basis of the observations above, here we put forward a hypothesis that integrates many of the suspected early-acting factors into flow-based symmetry breakage (Fig. 6). We hypothesize that serotonin enrichment in superficial cells of the blastula is a prerequisite of SM specification, as it allows for canonical Wnt signaling, and that it results from apical localization of serotonin prior to tangential cleavage divisions (Chalmers et al., 2005, 2003; Hausen and Riebesell, 1991). These tangential divisions begin at the 64-cell stage, persist through stage 9 and generate two new cell types: outer epithelial cells and inner non-epithelial cells. The outer cell layer becomes connected by true apical junctional complexes, including tight and adherens junctions (Chalmers et al., 2005, 2003; Fesenko et al., 2000; Hausen and Riebesell, 1991; Merzdorf et al., 1998; Müller and Hausen, 1995). We envisage the following scenario (Fig. 6): motor proteins (likely Kif16b; Hoepfner et al., 2005) move serotonin-loaded vesicles along microtubules to the apical surfaces of cells. Tangential cleavages (Chalmers et al., 2003, 2005) would then effectively sequester serotonin in the outer cell layer. Cytoplasmic re-uptake upon

Table 4
Frequencies of LR defects upon manipulation of presumed early determinants vs. Coco.

Factor	Treatment	Frequency (%)	References
Ion channels	Various inhibitors	15–51	Adams et al. (2006), Aw et al. (2010, 2008), Levin et al. (2002) and Morokuma et al. (2008)
	Various mRNA injections	9–44	
Serotonin signaling	Various inhibitors	10–44	Fukumoto et al. (2005b, 2005a), Rea et al. (2013) and Vandenberg et al. (2013a)
	Various mRNA injections	11–56	
cytoskeleton	Various inhibitors	19–38	Lobikin et al. (2012) and Qiu et al. (2005)
	Various mRNA injections	8–32.5 ^a	
Other factors	Various inhibitors	22.5–25 ^b	Bunney et al. (2003), Carneiro et al. (2011) and Vandenberg and Levin (2013, 2012)
	Various mRNA injections	5–75	
Coco	MO-mediated Knockdown (right)	70–98	Schweickert et al. (2010), Tingler et al. (2014) and Vonica and Brivanlou (2007)
	DNA or mRNA injections (left)	83–100	

^a Excluding one outlier experiment with one construct (tub4a; Lobikin et al., 2012), which caused misexpression of *Nodal* in 64.7% of cases (cf. Table S3).

^b Excluding one part of a NaB-HDAC-inhibitor experiment which caused misexpression of *Nodal* in 64% of an unknown number of cases (cf. Table S4).

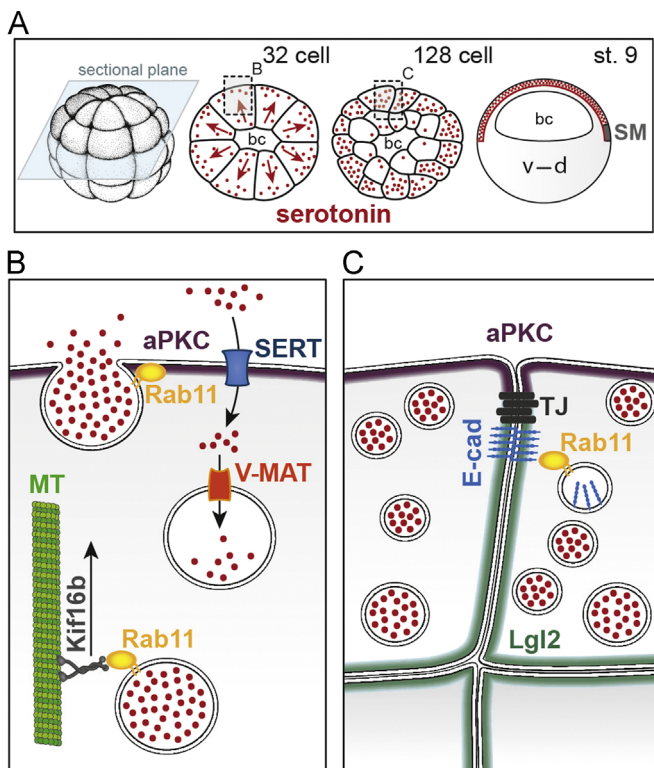


Fig. 6. Hypothesis: “early” determinants are required for SM specification through serotonin accumulation in epithelial cells. (A) Schematic depiction of serotonin accumulation in the epithelial layer of the blastocoel roof before the onset of gastrulation. Transversal sections of 32- and 128-cell embryos (plane indicated in light blue) and sagittal (animal–vegetal) section of stage 9 blastula embryo. bc, Blastocoel; d, dorsal; v, ventral. Redrawn from (Beyer et al., 2012a; Vandenberg and Levin, 2010b). (B) Apical enrichment of serotonin through Rab11/Kif16b/microtubule (MT) mediated exocytosis, re-uptake through SERT and re-packaging into vesicles through V-MAT. (C) Epithelialization of the outer layer of the blastula. For details see text.

secretion through the serotonin transporter SERT and sequestration into vesicles through the vesicular monoamine transporter VMAT would likely enhance accumulation in outer cells. Rab11 might function in cargo recognition, vesicle secretion and epithelialization (Jing and Prekeris, 2009). [We recently re-evaluated the function of Rab11. Efficiencies were low and differences between 1- and 4-cell manipulations, a prediction of the ion-flux model, were not found (Tingler et al., 2014)]. Microtubules, rab GTPases, SERT, VMAT and the tight junctional protein claudin have been previously implicated as “early” determinants (Vandenberg and Levin, 2013). Thus, the possibility that these components are actual players at much later stages needs to be tested in the context of serotonin accumulation

and SM specification. Some of the previously described phenotypes support this assumption. In claudin-manipulated embryos, for example, the epithelial organization of the blastula was disturbed (Brizuela et al., 2001). Our hypothesis is testable and should prove or disprove itself with further investigations. The ion-flux model, in contrast, features very early events and very late readouts, with mechanistic testing remaining to be done in between.

Open questions

Some important open questions remain. Symmetry breakage in chick, where the molecular analysis of laterality began with the 1995 landmark paper (Levin et al., 1995), and which allowed this field to erupt beyond the speculative into the direct experimental and mechanistic discovery phase, is far from solved. It is clear, however, that ATP4 plays a central role upstream of chiral cell migration (Gros et al., 2009), as it does in the sea urchin larva, upstream of the *Nodal* cascade (Bessodes et al., 2012). This gene, perhaps, might function as an entry point to elucidate the evolution of asymmetry (Blum et al., 2014). Other major challenges lie in the elucidation of the mechanisms of flow sensing and signal transfer to the left LPM. Answers will come from studying and comparing the different vertebrate model organisms, and perhaps extending analyses to new ones, such as reptiles.

Concluding remarks

All available evidence supports flow at the LRO as the single instructive event that breaks symmetry in fish, amphibians and mammals. Stochastic selection by any individual embryo between multiple co-existing modes of symmetry breakage, an idea recently voiced (Vandenberg and Levin, 2013), seems unlikely based on evolutionary reasoning, and without a plausible decision-making mechanism, seems uncomfortably teleological. Maintaining fully functional but highly divergent complex mechanisms (ion flux, flow, others) to achieve the very same result (*situs solitus*) in our understanding should impact on evolutionary fitness and be heavily selected against. As flow occurs relatively late (neurula) and requires elaborate structures (ciliated epithelium, sensor, extracellular ligand transfer), it should be not surprising that earlier morphogenetic events or processes involved in inducing or actually physically constructing the organizer and LRO tissues have an impact on flow. Future experiments should reveal the exact roles of the factors in question and whether they are functionally conserved in the various model organisms.

Acknowledgments

We are grateful to Rebecca Burdine (Princeton) and Cecilia Lo (Pittsburgh) for sharing unpublished results and observations. The generous help from Matthias Tisler and Tim Ott in preparing all figures was much appreciated and is gratefully acknowledged. Work in the Blum lab was supported by DFG Grants BL285/9-2 and BL285/10-1, PV was the recipient of a DFG return fellowship (VI-574/2-1), and CW was supported by NIH R01-GM56238.

Appendix A. Supporting information

Supplementary data associated with this article can be found in the online version at <http://dx.doi.org/10.1016/j.ydbio.2014.06.014>.

References

- Adams, D.S., Robinson, K.R., Fukumoto, T., Yuan, S., Albertson, R.C., Yelick, P., Kuo, L., McSweeney, M., Levin, M., 2006. Early, H⁺-V-ATPase-dependent proton flux is necessary for consistent left–right patterning of non-mammalian vertebrates. *Development* 133, 1657–1671.
- Aizawa, H., 2013. Habenula and the asymmetric development of the vertebrate brain. *Anat. Sci. Int.* 88, 1–9.
- Amack, J.D., Yost, H.J., 2004. The T box transcription factor no tail in ciliated cells controls zebrafish left–right asymmetry. *Curr. Biol.* 14, 685–690.
- Aw, S., Adams, D.S., Qiu, D., Levin, M., 2008. H,K-ATPase protein localization and Kir4.1 function reveal concordance of three axes during early determination of left–right asymmetry. *Mech. Dev.* 125, 353–372.
- Aw, S., Koster, J.C., Pearson, W., Nichols, C.G., Shi, N.-Q., Carneiro, K., Levin, M., 2010. The ATP-sensitive K(+)–channel (K(ATP)) controls early left–right patterning in *Xenopus* and chick embryos. *Dev. Biol.* 346, 39–53.
- Bajoghli, B., Aghaallaei, N., Soroldoni, D., Czerny, T., 2007. The roles of Groucho/Tle in left–right asymmetry and Kupffer's vesicle organogenesis. *Dev. Biol.* 303, 347–361.
- Bartram, U., Wirbelauer, J., Speer, C.P., 2005. Heterotaxy syndrome – asplenia and polysplenia as indicators of visceral malposition and complex congenital heart disease. *Biol. Neonate* 88, 278–290.
- Basu, B., Brueckner, M., 2008. Cilia multifunctional organelles at the center of vertebrate left–right asymmetry. *Curr. Top. Dev. Biol.* 85, 151–174.
- Bessodes, N., Haillet, E., Duboc, V., Röttinger, E., Lahaye, F., Lepage, T., 2012. Reciprocal signaling between the ectoderm and a mesendodermal left–right organizer directs left–right determination in the sea urchin embryo. *PLoS Genet.* 8, e1003121.
- Beyer, T., Danilchik, M., Thumberger, T., Vick, P., Tisler, M., Schneider, I., Bogusch, S., Andre, P., Ulmer, B., Walentek, P., Niesler, B., Blum, M., Schweickert, A., 2012a. Serotonin signaling is required for Wnt-dependent GRP specification and leftward flow in *Xenopus*. *Curr. Biol.* 22, 33–39.
- Beyer, T., Thumberger, T., Schweickert, A., Blum, M., 2012b. Connexin26-mediated transfer of laterality cues in *Xenopus*. *Biol. Open* 1, 473–481.
- Biggrove, B.W., Essner, J.J., Yost, H.J., 1999. Regulation of midline development by antagonism of lefty and nodal signaling. *Development* 126, 3253–3262.
- Biggrove, B.W., Essner, J.J., Yost, H.J., 2000. Multiple pathways in the midline regulate concordant brain, heart and gut left–right asymmetry. *Development* 127, 3567–3579.
- Biggrove, B.W., Morelli, S.H., Yost, H.J., 2003. Genetics of human laterality disorders: insights from vertebrate model systems. *Annu. Rev. Genomics Hum. Genet.* 4, 1–32.
- Blum, M., Andre, P., Muders, K., Schweickert, A., Fischer, A., Bitzer, E., Bogusch, S., Beyer, T., van Straaten, H.W.M., Viebahn, C., 2007. Ciliation and gene expression distinguish between node and posterior notochord in the mammalian embryo. *Differentiation* 75, 133–146.
- Blum, M., Beyer, T., Weber, T., Vick, P., Andre, P., Bitzer, E., Schweickert, A., 2009a. *Xenopus*, an ideal model system to study vertebrate left–right asymmetry. *Dev. Dyn.* 238, 1215–1225.
- Blum, M., Weber, T., Beyer, T., Vick, P., 2009b. Evolution of leftward flow. *Semin. Cell Dev. Biol.* 20, 464–471.
- Blum, M., Feistel, K., Thumberger, T., Schweickert, A., 2014. The evolution and conservation of left–right patterning mechanisms. *Development* 141, 1603–1613.
- Brizuela, B.J., Wessely, O., De Robertis, E.M., 2001. Overexpression of the *Xenopus* tight-junction protein claudin causes randomization of the left–right body axis. *Dev. Biol.* 230, 217–229.
- Brown, N.A., Wolpert, L., 1990. The development of handedness in left/right asymmetry. *Development* 109, 1–9.
- Bunney, T.D., De Boer, A.H., Levin, M., 2003. Fusicoccin signaling reveals 14–3-3 protein function as a novel step in left–right patterning during amphibian embryogenesis. *Development* 130, 4847–4858.
- Burdine, R.D., Caspary, T., 2013. Left–right asymmetry: lessons from *Cancun*. *Development* 140, 4465–4470.
- Burn, S.F., Hill, R.E., 2009. Left–right asymmetry in gut development: what happens next? *Bioessays* 31, 1026–1037.
- Carneiro, K., Donnet, C., Rejtar, T., Karger, B.L., Barisone, G.A., Díaz, E., Kortagere, S., Lemire, J.M., Levin, M., 2011. Histone deacetylase activity is necessary for left–right patterning during vertebrate development. *BMC Dev. Biol.* 11, 29.
- Chalmers, A.D., Pambos, M., Mason, J., Lang, S., Wylie, C., Papalopulu, N., 2005. aPKC, Crumbs3 and Lgl2 control apical polarity in early vertebrate development. *Development* 132, 977–986.
- Chalmers, A.D., Strauss, B., Papalopulu, N., 2003. Oriented cell divisions asymmetrically segregate aPKC and generate cell fate diversity in the early *Xenopus* embryo. *Development* 130, 2657–2668.
- Chea, H.K., Wright, C.V., Swalla, B.J., 2005. Nodal signaling and the evolution of deuterostome gastrulation. *Dev. Dyn.* 234, 269–278.
- Chen, J.N., van Bebber, F., Goldstein, A.M., Serluca, F.C., Jackson, D., Childs, S., Serbedzija, G., Warren, K.S., Mably, J.D., Lindahl, P., Mayer, A., Haftter, P., Fishman, M.C., 2001. Genetic steps to organ laterality in zebrafish. *Comp. Funct. Genomics* 2, 60–68.
- Cheng, A.M., Thisse, B., Thisse, C., Wright, C.V., 2000. The lefty-related factor *Xatv* acts as a feedback inhibitor of nodal signaling in mesoderm induction and L–R axis development in *Xenopus*. *Development* 127, 1049–1061.
- Danilchik, M.V., Brown, E.E., Riegl, K., 2006. Intrinsic chiral properties of the *Xenopus* egg cortex: an early indicator of left–right asymmetry? *Development* 133, 4517–4526.
- Danos, M.C., Yost, H.J., 1995. Linkage of cardiac left–right asymmetry and dorsal–anterior development in *Xenopus*. *Development* 121, 1467–1474.
- Danos, M.C., Yost, H.J., 1996. Role of notochord in specification of cardiac left–right orientation in Zebrafish and *Xenopus*. *Dev. Biol.* 177, 96–103.
- Dathe, V., Gamel, A., Männer, J., Brand-Saberi, B., Christ, B., 2002. Morphological left–right asymmetry of Hensen's node precedes the asymmetric expression of *Shh* and *Fgf8* in the chick embryo. *Anat. Embryol.* 205, 343–354.
- De Robertis, E.M., Larraín, J., Oelgeschläger, M., Wessely, O., 2000. The establishment of Spemann's organizer and patterning of the vertebrate embryo. *Nat. Rev. Genet.* 1, 171–181.
- Ermakov, A., Stevens, J.L., Whitehill, E., Robson, J.E., Pieves, G., Brooker, D., Gogolidou, P., Powles-Glover, N., Hacker, T., Young, S.R., Dear, N., Hirst, E., Tymowska-Lalanne, Z., Briscoe, J., Bhattacharya, S., Norris, D.P., 2009. Mouse mutagenesis identifies novel roles for left–right patterning genes in pulmonary, craniofacial, ocular, and limb development. *Dev. Dyn.* 238, 581–594.
- Essner, J.J., Amack, J.D., Nyholm, M.K., Harris, E.B., Yost, H.J., 2005. Kupffer's vesicle is a ciliated organ of asymmetry in the zebrafish embryo that initiates left–right development of the brain, heart and gut. *Development* 132, 1247–1260.
- Fan, M.J., Sokol, S.Y., 1997. A role for Siamois in Spemann organizer formation. *Development* 124, 2581–2589.
- Feistel, K., 2007. Determination of Laterality in the Rabbit Embryo: Studies on Ciliation and Asymmetric Signal Transfer. (<https://opus.uni-hohenheim.de/volltexte/2007/177/>).
- Fesenko, I., Kurth, T., Sheth, B., Fleming, T.P., Citi, S., Hausen, P., 2000. Tight junction biogenesis in the early *Xenopus* embryo. *Mech. Dev.* 96, 51–65.
- Field, S., Riley, K.-L., Grimes, D.T., Hilton, H., Simon, M., Powles-Glover, N., Siggers, P., Bogani, D., Greenfield, A., Norris, D.P., 2011. *Pkd11* establishes left–right asymmetry and physically interacts with *Pkd2*. *Development* 138, 1131–1142.
- Franco, D., Christoffels, V.M., Campione, M., 2014. Homeobox transcription factor *Pitx2*: the rise of an asymmetry gene in cardiogenesis and arrhythmogenesis. *Trends Cardiovasc. Med.* 24, 23–31.
- Fukumoto, T., Blakely, R., Levin, M., 2005a. Serotonin transporter function is an early step in left–right patterning in chick and frog embryos. *Dev. Neurosci.* 27, 349–363.
- Fukumoto, T., Kema, I.P., Levin, M., 2005b. Serotonin signaling is a very early step in patterning of the left–right axis in chick and frog embryos. *Curr. Biol.* 15, 794–803.
- Gerhart, J., Danilchik, M., Doniach, T., Roberts, S., Rowning, B., Stewart, R., 1989. Cortical rotation of the *Xenopus* egg: consequences for the anteroposterior pattern of embryonic dorsal development. *Development* 107 (Suppl.), S37–S51.
- Grande, C., Patel, N.H., 2009. Nodal signalling is involved in left–right asymmetry in snails. *Nature* 457, 1007–1011.
- Gros, J., Feistel, K., Viebahn, C., Blum, M., Tabin, C.J., 2009. Cell movements at Hensen's node establish left/right asymmetric gene expression in the chick. *Science* 324, 941–944.
- Guthrie, S.C., 1984. Patterns of junctional communication in the early amphibian embryo. *Nature* 311, 149–151.
- Hamada, H., Meno, C., Watanabe, D., Saijoh, Y., 2002. Establishment of vertebrate left–right asymmetry. *Nat. Rev. Genet.* 3, 103–113.
- Hausen, P., Riebesell, M., 1991. *The Early Development of Xenopus laevis*. Springer-Verlag, Berlin, Heidelberg, New York.
- Hirokawa, N., Tanaka, Y., Okada, Y., 2012. Cilia, KIF3 molecular motor and nodal flow. *Curr. Opin. Cell Biol.* 24, 31–39.
- Hoepfner, S., Severin, F., Cabezas, A., Habermann, B., Runge, A., Gillyooly, D., Stenmark, H., Zerial, M., 2005. Modulation of receptor recycling and degradation by the endosomal kinesin KIF16B. *Cell* 121, 437–450.
- Hoyo, M., Takashima, S., Kobayashi, D., Sumeragi, A., Shimada, A., Tsukahara, T., Yokoi, H., Narita, T., Jindo, T., Kage, T., Kitagawa, T., Kimura, T., Sekimizu, K., Miyake, A., Setiamarga, D., Murakami, R., Tsuda, S., Ooki, S., Kakihara, K., Naruse, K., Takeda, H., 2007. Right-elevated expression of *charon* is regulated by fluid flow in medaka Kupffer's vesicle. *Dev. Growth Differ.* 49, 395–405.

- Izraeli, S., Lowe, L.A., Bertness, V.L., Good, D.J., Dorward, D.W., Kirsch, I.R., Kuehn, M.R., 1999. The *SIL* gene is required for mouse embryonic axial development and left-right specification. *Nature* 399, 691–694.
- Jing, J., Prekeris, R., 2009. Polarized endocytic transport: the roles of Rab11 and Rab11-FIPs in regulating cell polarity. *Histol. Histopathol.* 24, 1171–1180.
- Kao, K.R., Elinson, R.P., 1988. The entire mesodermal mantle behaves as Spemann's organizer in dorsoanterior enhanced *Xenopus laevis* embryos. *Dev. Biol.* 127, 64–77.
- King, T., Beddington, R.S., Brown, N.A., 1998. The role of the *brachyury* gene in heart development and left-right specification in the mouse. *Mech. Dev.* 79, 29–37.
- Kramer-Zucker, A.G., Olale, F., Haycraft, C.J., Yoder, B.K., Schier, A.F., Drummond, I.A., 2005. Cilia-driven fluid flow in the zebrafish pronephros, brain and Kupffer's vesicle is required for normal organogenesis. *Development* 132, 1907–1921.
- Ku, M., Melton, D.A., 1993. *Xwnt-11*: a maternally expressed *Xenopus wnt* gene. *Development* 119, 1161–1173.
- Landesman, Y., Goodenough, D.A., Paul, D.L., 2000. Gap junctional communication in the early *Xenopus* embryo. *J. Cell Biol.* 150, 929–936.
- Lee, J.D., Anderson, K.V., 2008. Morphogenesis of the node and notochord: the cellular basis for the establishment and maintenance of left-right asymmetry in the mouse. *Dev. Dyn.* 237, 3464–3476.
- Lenhart, K.F., Lin, S.-Y., Titus, T.A., Postlethwait, J.H., Burdine, R.D., 2011. Two additional midline barriers function with midline *lefty1* expression to maintain asymmetric Nodal signaling during left-right axis specification in zebrafish. *Development* 138, 4405–4410.
- Levin, M., 2005. Left-right asymmetry in embryonic development: a comprehensive review. *Mech. Dev.* 122, 3–25.
- Levin, M., Johnson, R.L., Sterna, C.D., Kuehn, M., Tabin, C., 1995. A molecular pathway determining left-right asymmetry in chick embryogenesis. *Cell* 82, 803–814.
- Levin, M., Mercola, M., 1998. Gap junctions are involved in the early generation of left-right asymmetry. *Dev. Biol.* 203, 90–105.
- Levin, M., Mercola, M., 1999. Gap junction-mediated transfer of left-right patterning signals in the early chick blastoderm is upstream of *Shh* asymmetry in the node. *Development* 126, 4703–4714.
- Levin, M., Thorlin, T., Robinson, K.R., Nogi, T., Mercola, M., 2002. Asymmetries in H^+/K^+ -ATPase and cell membrane potentials comprise a very early step in left-right patterning. *Cell* 111, 77–89.
- Li, E., Materna, S.C., Davidson, E.H., 2012. Direct and indirect control of oral ectoderm regulatory gene expression by Nodal signaling in the sea urchin embryo. *Dev. Biol.* 369, 377–385.
- Li, E., Materna, S.C., Davidson, E.H., 2013. New regulatory circuit controlling spatial and temporal gene expression in the sea urchin embryo oral ectoderm GRN. *Dev. Biol.* 382, 268–279.
- Liu, X., Tobita, K., Francis, R.J.B., Lo, C.W., 2013. Imaging techniques for visualizing and phenotyping congenital heart defects in murine models. *Birth Defects Res. C: Embryo Today* 99, 93–105.
- Lobikin, M., Wang, G., Xu, J., Hsieh, Y.-W., Chuang, C.-F., Lemire, J.M., Levin, M., 2012. Early, nonciliary role for microtubule proteins in left-right patterning is conserved across kingdoms. *Proc. Natl. Acad. Sci. USA* 109, 12586–12591.
- Lohr, J.L., Danos, M.C., Yost, H.J., 1997. Left-right asymmetry of a nodal-related gene is regulated by dorsoanterior midline structures during *Xenopus* development. *Development* 124, 1465–1472.
- Marjoram, L., Wright, C., 2011. Rapid differential transport of Nodal and *Lefty* on sulfated proteoglycan-rich extracellular matrix regulates left-right asymmetry in *Xenopus*. *Development* 138, 475–485.
- Marques, S., Borges, A.C., Silva, A.C., Freitas, S., Cordenonsi, M., Belo, J.A., 2004. The activity of the Nodal antagonist *Cerl-2* in the mouse node is required for correct L/R body axis. *Genes Dev.* 18, 2342–2347.
- McGrath, J., Brueckner, M., 2003. Cilia are at the heart of vertebrate left-right asymmetry. *Curr. Opin. Genet. Dev.* 13, 385–392.
- Melloy, P.G., Ewart, J.L., Cohen, M.F., Desmond, M.E., Kuehn, M.R., Lo, C.W., 1998. No turning, a mouse mutation causing left-right and axial patterning defects. *Dev. Biol.* 193, 77–89.
- Merzdorf, C.S., Chen, Y.H., Goodenough, D.A., 1998. Formation of functional tight junctions in *Xenopus* embryos. *Dev. Biol.* 195, 187–203.
- Miller, J.R., Rowning, B.A., Larabell, C.A., Yang-Snyder, J.A., Bates, R.L., Moon, R.T., 1999. Establishment of the dorsal-ventral axis in *Xenopus* embryos coincides with the dorsal enrichment of dishevelled that is dependent on cortical rotation. *J. Cell Biol.* 146, 427–437.
- Molina, M.D., de Crozé, N., Hailott, E., Lepage, T., 2013. Nodal: master and commander of the dorsal. *Curr. Opin. Genet. Dev.* 23, 445–453.
- Morokuma, J., Blackiston, D., Levin, M., 2008. *KCNQ1* and *KCNE1* K^+ channel components are involved in early left-right patterning in *Xenopus laevis* embryos. *Cell. Physiol. Biochem.* 21, 357–372.
- Müller, H.A., Hausen, P., 1995. Epithelial cell polarity in early *Xenopus* development. *Dev. Dyn.* 202, 405–420.
- Nakamura, T., Hamada, H., 2012. Left-right patterning: conserved and divergent mechanisms. *Development* 139, 3257–3262.
- Nakamura, T., Saito, D., Kawasumi, A., Shinohara, K., Asai, Y., Takaoka, K., Dong, F., Takamatsu, A., Belo, J.A., Mochizuki, A., Hamada, H., 2012. Fluid flow and interlinked feedback loops establish left-right asymmetric decay of *Cerl2* mRNA. *Nat. Commun.* 3, 1322.
- Nascone, N., Mercola, M., 1997. Organizer induction determines left-right asymmetry in *Xenopus*. *Dev. Biol.* 189, 68–78.
- Nonaka, S., Tanaka, Y., Okada, Y., Takeda, S., Harada, A., Kanai, Y., Kido, M., Hirokawa, N., 1998. Randomization of left-right asymmetry due to loss of nodal cilia generating leftward flow of extraembryonic fluid in mice lacking *KIF3B* motor protein. *Cell* 95, 829–837.
- Norris, D.P., Grimes, D.T., 2012. Mouse models of ciliopathies: the state of the art. *Dis. Model. Mech.* 5, 299–312.
- Oh, E.C., Katsanis, N., 2012. Cilia in vertebrate development and disease. *Development* 139, 443–448.
- Ohi, Y., Wright, C.V.E., 2007. Anteriorward shifting of asymmetric *Xnr1* expression and contralateral communication in left-right specification in *Xenopus*. *Dev. Biol.* 301, 447–463.
- Okada, Y., Takeda, S., Tanaka, Y., Belmonte, J.-C.I., Hirokawa, N., 2005. Mechanism of nodal flow: a conserved symmetry breaking event in left-right axis determination. *Cell* 121, 633–644.
- Panizzi, J.R., Becker-Heck, A., Castleman, V.H., Al-Mutairi, D.A., Liu, Y., Loges, N.T., Pathak, N., Austin-Tse, C., Sheridan, E., Schmidts, M., Olbrich, H., Werner, C., Häffner, K., Hellman, N., Chodhari, R., Gupta, A., Kramer-Zucker, A., Olale, F., Burdine, R.D., Schier, A.F., O'Callaghan, C., Chung, E.M.K., Reinhardt, R., Mitchison, H.M., King, S.M., Omran, H., Drummond, I.A., 2012. *CCDC103* mutations cause primary ciliary dyskinesia by disrupting assembly of ciliary dynein arms. *Nat. Genet.* 44, 714–719.
- Peeters, H., Devriendt, K., 2006. Human laterality disorders. *Eur. J. Med. Genet.* 49, 349–362.
- Perloff, J.K., 2011. The cardiac malpositions. *Am. J. Cardiol.* 108, 1352–1361.
- Qiu, D., Cheng, S.-M., Wozniak, L., McSweeney, M., Perrone, E., Levin, M., 2005. Localization and loss-of-function implicates ciliary proteins in early, cytoplasmic roles in left-right asymmetry. *Dev. Dyn.* 234, 176–189.
- Raya, A., Izpisua-Belmonte, J.C., 2004. Unveiling the establishment of left-right asymmetry in the chick embryo. *Mech. Dev.* 121, 1043–1054.
- Rea, A.C., Vandenberg, L.N., Ball, R.E., Snouffer, A.A., Hudson, A.G., Zhu, Y., McLain, D.E., Johnston, L.L., Lauderdale, J.D., Levin, M., Dore, T.M., 2013. Light-activated serotonin for exploring its action in biological systems. *Chem. Biol.* 20, 1536–1546.
- Roussigne, M., Blader, P., Wilson, S.W., 2012. Breaking symmetry: the zebrafish as a model for understanding left-right asymmetry in the developing brain. *Dev. Neurobiol.* 72, 269–281.
- Rutenberg, J., Cheng, S.-M., Levin, M., 2002. Early embryonic expression of ion channels and pumps in chick and *Xenopus* development. *Dev. Dyn.* 225, 469–484.
- Scharf, S.R., Gerhart, J.C., 1980. Determination of the dorsal-ventral axis in eggs of *Xenopus laevis*: complete rescue of uv-impaired eggs by oblique orientation before first cleavage. *Dev. Biol.* 79, 181–198.
- Schier, A.F., 2009. Nodal morphogens. *Cold Spring Harb. Perspect. Biol.* 1, a003459.
- Schottenfeld, J., Sullivan-Brown, J., Burdine, R.D., 2007. Zebrafish curly up encodes a *Pkd2* ortholog that restricts left-side-specific expression of southpaw. *Development* 134, 1605–1615.
- Schulte-Merker, S., van Eeden, F.J., Halpern, M.E., Kimmel, C.B., Nüsslein-Volhard, C., 1994. No tail (*ntl*) is the zebrafish homologue of the mouse *T* (*Brachyury*) gene. *Development* 120, 1009–1015.
- Schweickert, A., Vick, P., Getwan, M., Weber, T., Schneider, I., Eberhardt, M., Beyer, T., Pachur, A., Blum, M., 2010. The nodal inhibitor *coco* is a critical target of leftward flow in *Xenopus*. *Curr. Biol.* 20, 738–743.
- Schweickert, A., Walentek, P., Thumberger, T., Danilchik, M., 2012. Linking early determinants and cilia-driven leftward flow in left-right axis specification of *Xenopus laevis*: a theoretical approach. *Differentiation* 83, S67–S77.
- Schweickert, A., Weber, T., Vick, P., Bogusch, S., Feistel, K., Blum, M., 2007. Cilia-driven leftward flow determines laterality in *Xenopus*. *Curr. Biol.* 17, 60–66.
- Serluca, F.C., Xu, B., Okabe, N., Baker, K., Lin, S.-Y., Sullivan-Brown, J., Konieczkowski, D. J., Jaffe, K.M., Bradner, J.M., Fishman, M.C., Burdine, R.D., 2009. Mutations in zebrafish leucine-rich repeat-containing six-like affect cilia motility and result in pronephric cysts, but have variable effects on left-right patterning. *Development* 136, 1621–1631.
- Shen, M.M., 2007. Nodal signaling: developmental roles and regulation. *Development* 134, 1023–1034.
- Shiraishi, I., Ichikawa, H., 2012. Human heterotaxy syndrome – from molecular genetics to clinical features, management, and prognosis. *Circ. J.* 76, 2066–2075.
- Shiratori, H., Hamada, H., 2006. The left-right axis in the mouse: from origin to morphology. *Development* 133, 2095–2104.
- Shook, D.R., Majer, C., Keller, R., 2004. Pattern and morphogenesis of presumptive superficial mesoderm in two closely related species, *Xenopus laevis* and *Xenopus tropicalis*. *Dev. Biol.* 270, 163–185.
- Sokol, S., Christian, J.L., Moon, R.T., Melton, D.A., 1991. Injected *Wnt* RNA induces a complete body axis in *Xenopus* embryos. *Cell* 67, 741–752.
- Stubbs, J.L., Oishi, I., Izpisua-Belmonte, J.C., Kintner, C., 2008. The forkhead protein *Foxj1* specifies node-like cilia in *Xenopus* and zebrafish embryos. *Nat. Genet.* 40, 1454–1460.
- Sullivan-Brown, J., Schottenfeld, J., Okabe, N., Hostetter, C.L., Serluca, F.C., Thiberge, S.Y., Burdine, R.D., 2008. Zebrafish mutations affecting cilia motility share similar cystic phenotypes and suggest a mechanism of cyst formation that differs from *pkd2* morphants. *Dev. Biol.* 314, 261–275.
- Sun, Z., Amsterdam, A., Pazour, G.J., Cole, D.G., Miller, M.S., Hopkins, N., 2004. A genetic screen in zebrafish identifies cilia genes as a principal cause of cystic kidney. *Development* 131, 4085–4093.
- Sutherland, M.J., Ware, S.M., 2009. Disorders of left-right asymmetry: heterotaxy and situs inversus. *Am. J. Med. Genet. C: Semin. Med. Genet.* 151C, 307–317.
- Tao, Q., Yokota, C., Puck, H., Kofron, M., Birsoy, B., Yan, D., Asashima, M., Wylie, C.C., Lin, X., Heasman, J., 2005. Maternal *wnt11* activates the canonical *wnt* signaling pathway required for axis formation in *Xenopus* embryos. *Cell* 120, 857–871.

- Tingler, M., Ott, T., Tözser, J., Getwan, M., Kurz, S., Tisler, M., Schweickert, A., Blum, M., 2014. Symmetry breakage in the frog *Xenopus*: role of Rab11 and the ventral-right blastomere. *Genesis* 52, 588–599.
- Vandenberg, L.N., 2012. Laterality defects are influenced by timing of treatments and animal model. *Differentiation* 83, 26–37.
- Vandenberg, L.N., Lemire, J.M., Levin, M., 2013a. Serotonin has early, cilia-independent roles in *Xenopus* left–right patterning. *Dis. Model. Mech.* 6, 261–268.
- Vandenberg, L.N., Levin, M., 2010a. Far from solved: a perspective on what we know about early mechanisms of left–right asymmetry. *Dev. Dyn.* 239, 3131–3146.
- Vandenberg, L.N., Levin, M., 2010b. Consistent left–right asymmetry cannot be established by late organizers in *Xenopus* unless the late organizer is a conjoined twin. *Development* 137, 1095–1105.
- Vandenberg, L.N., Levin, M., 2012. Polarity proteins are required for left–right axis orientation and twin–twin instruction. *Genesis* 50, 219–234.
- Vandenberg, L.N., Levin, M., 2013. A unified model for left–right asymmetry? Comparison and synthesis of molecular models of embryonic laterality. *Dev. Biol.* 379, 1–15.
- Vandenberg, L.N., Morrie, R.D., Seebohm, G., Lemire, J.M., Levin, M., 2013b. Rab GTPases are required for early orientation of the left–right axis in *Xenopus*. *Mech. Dev.* 130, 254–271.
- Vincent, J.-P., Oster, G.F., Gerhart, J.C., 1986. Kinematics of gray crescent formation in *Xenopus* eggs: the displacement of subcortical cytoplasm relative to the egg surface. *Dev. Biol.* 113, 484–500.
- Viotti, M., Niu, L., Shi, S.-H., Hadjantonakis, A.-K., 2012. Role of the gut endoderm in relaying left–right patterning in mice. *PLoS Biol.* 10, e1001276.
- Vonica, A., Brivanlou, A.H., 2007. The left–right axis is regulated by the interplay of *Coco*, *Xnr1* and *derrière* in *Xenopus* embryos. *Dev. Biol.* 303, 281–294.
- Walentek, P., Beyer, T., Thumberger, T., Schweickert, A., Blum, M., 2012. ATP4a is required for Wnt-dependent *Foxj1* expression and leftward flow in *Xenopus* left–right development. *Cell Rep.* 1, 516–527.
- Weaver, C., Kimelman, D., 2004. Move it or lose it: axis specification in *Xenopus*. *Development* 131, 3491–3499.
- Wetzel, R., 1929. Untersuchungen am Hühnchen. Die Entwicklung des Keims während der ersten beiden Bruttage. *Arch. Entwicklungsmechanik Org.* 119, 188–321.
- Wilkinson, D.G., Bhatt, S., Herrmann, B.G., 1990. Expression pattern of the mouse *T* gene and its role in mesoderm formation. *Nature* 343, 657–659.
- Yoshida, S., Hamada, H., 2014. Roles of cilia, fluid flow, and Ca^{2+} signaling in breaking of left–right symmetry. *Trends Genet.* 30, 10–17.
- Zhang, J., King, M.L., 1996. *Xenopus* *VegT* RNA is localized to the vegetal cortex during oogenesis and encodes a novel T-box transcription factor involved in mesodermal patterning. *Development* 122, 4119–4129.
- Zhang, M., Zhang, J., Lin, S.C., Meng, A., 2012. Catenin 1 and catenin 2 play similar and distinct roles in left–right asymmetric development of zebrafish embryos. *Development* 139, 2009–2019.